

1 **IMPACT OF VARYING COMMUNITY NETWORKS ON DISEASE**
2 **INVASION***

3 STEPHEN KIRKLAND[†], ZHISHENG SHUAI[‡], P. VAN DEN DRIESSCHE[§], AND XUEYING
4 WANG[¶]

5 **Abstract.** We consider the spread of an infectious disease in a heterogeneous environment,
6 modelled as a network of patches. We focus on the invasibility of the disease, as quantified by the
7 corresponding value of an approximation to the network basic reproduction number, \mathcal{R}_0 , and study
8 how changes in the network structure affect the value of \mathcal{R}_0 . We provide a detailed analysis for two
9 model networks, a star and a path, and discuss the changes to the corresponding network structure
10 that yield the largest decrease in \mathcal{R}_0 . We develop both combinatorial and matrix analytic techniques,
11 and illustrate our theoretical results by simulations with the exact \mathcal{R}_0 .

12 **Key words.** Basic reproduction number; Matrix–Tree theorem; Group inverse.

13 **AMS subject classifications.** 92D30, 92D25, 15A09, 15A18.

14 **1. Introduction.** Advanced science and technology have made our world an in-
15 creasingly connected place. Globalization and urbanization bring not only benefits,
16 but also attendant consequences such as the spread of emerging and re-emerging infec-
17 tious diseases. Historically, plague, cholera and influenza have resulted in millions of
18 human deaths, and insight into the spread and control of these diseases has shaped our
19 modern society, particularly in medicine and public health. Recent emerging diseases
20 such as HIV/AIDS, SARS and Ebola highlight the need for scientific investigations
21 of disease spread via transport networks [43]. As disease vectors (e.g., mosquitoes
22 and ticks) can also be carried via human/goods transportation, the outbreak and
23 spread of vector-borne diseases such as dengue, Lyme disease, malaria, West Nile
24 virus, yellow fever, and Zika virus have exhibited strong spatio-temporal patterns
25 [15, 22, 26, 37, 40, 41, 42, 47] (also see the recent special issues [31, 39]), partly due
26 to the interplay between disease epidemiology and vector ecology. Spatio-temporal
27 patterns have also been observed for many waterborne diseases caused by pathogenic
28 micro-organisms such as bacteria and protozoa that are transmitted in water/river
29 networks [3, 20, 33, 38, 45, 46]. One of the main scientific challenges is to deter-
30 mine the connection between disease risk and the change of network structures (as a
31 consequence of human behavior and/or environmental uncertainty). Recent studies
32 using statistical data from climate, environmental and disease surveillance have shown
33 inconsistent and geographically variable results. For example, a discrepancy in the
34 correlation with precipitation has appeared in the literature of waterborne diseases:
35 a significant positive association between heavy rainfall and waterborne diseases is
36 often observed [9, 13, 16, 23, 32] (also see the review paper [30]), while increased
37 prevalence of waterborne diseases has also been reported as an unexpected conse-

*This work was partly funded by the NSERC Discovery Grants RGPIN–2019–05408 (SK) and RGPIN–3677–2016 (PvdD), the NSF Grant DMS-1716445 (ZS), and the Simons Foundation Grant 317407 (XW).

[†]Department of Mathematics, University of Manitoba, Winnipeg, MB, R3T 2N2, Canada (Stephen.Kirkland@umanitoba.ca).

[‡]Department of Mathematics, University of Central Florida, Orlando, FL 32816 (shuai@ucf.edu).

[§]Department of Mathematics and Statistics, University of Victoria, Victoria, BC, V8W 2Y2, Canada (pvdd@math.uvic.ca).

[¶]Department of Mathematics and Statistics, Washington State University, Pullman, WA 99164 (xueying@math.wsu.edu).

38 quence of drought [6] and the anthropogenic protection against annual flooding [10].
 39 Detailed discussions of this discrepancy, as a consequence of human behavior and/or
 40 climate change, have been surveyed in [4, 29], while rigorous scientific explanations
 41 and theoretical insights are lacking, due to the complexity and multiple time-scales.

42 Many existing studies in the literature have focused on the aggregation of disease
 43 dynamics at each geographical region (or patch) via a static movement (or commu-
 44 nity) network, either for the situation where the time scale of the dispersal among
 45 patches is much faster than the scale of patch demography/disease dynamics, or with
 46 the focus on monotonicity of disease invasibility with respect to dispersal speed or
 47 travel frequency; for example, see [1, 8, 17, 18, 19, 44]. Recently, a general result
 48 on the spectral monotonicity of a perturbed Laplacian matrix in [12] has provided a
 49 theoretical insight on the aggregation. Specifically, for a square matrix $A = Q - \mu L$,
 50 where $Q = \text{diag}\{q_k\}$ is a diagonal matrix encoding within-vertex (within-patch) pop-
 51 ulation/disease dynamics and L is a Laplacian matrix describing population dispersal
 52 among patches in a heterogeneous environment (of n patches), the monotonicity and
 53 convexity of the spectral abscissa of A , $s(A)$, with respect to dispersal speed μ is
 54 established: $\frac{ds(A)}{d\mu} \leq 0$ and $\frac{d^2s(A)}{d\mu^2} \geq 0$. The limiting behavior with a faster time
 55 scale of population/disease dynamics is like the decoupled (no movement) system,
 56 $s(A) = \max\{q_k\}$, while the limiting behavior with a faster time scale of dispersal is
 57 the u -weighted average, $s(A) = \sum_{k=1}^n u_k q_k$, where $u = (u_1, u_2, \dots, u_n)^\top$ is the nor-
 58 malized right null vector of L . As pointed out in [12], these results also are related
 59 to the reduction principle in evolution biology [2, 25] and the evolution of dispersal
 60 in patchy landscapes [27]. For many heterogeneous infectious disease models, the
 61 network basic reproduction number \mathcal{R}_0 , a threshold determining whether the disease
 62 dies out or persists, can be approximated as the u -weighted average of the individual
 63 patch reproduction numbers $\mathcal{R}_0^{(k)}$, $\mathcal{R}_0 = \sum_{k=1}^n u_k \mathcal{R}_0^{(k)}$, when the dispersal among
 64 geographic regions is faster than the disease/population dynamics; see, e.g., [17, 44]
 65 for waterborne diseases, [12, 19, 21] for general diseases of SIS or SIR type, and [8]
 66 for the analog in a continuous spatial landscape.

67 In this paper, we investigate the impact of varying community networks on disease
 68 invasion in a heterogeneous environment. Our motivation comes from the spread of a
 69 waterborne-disease such as cholera in a heterogeneous network, in which the pathogen
 70 (the bacterium *Vibrio cholerae*) moves along water in a hydrological landscape (e.g.,
 71 a river network) or the host moves between regions. If the network structure changes,
 72 our goal is to determine how this affects the network basic reproduction number \mathcal{R}_0
 73 for the spatial spread of the disease. The quantity \mathcal{R}_0 is important as it usually
 74 determines a threshold for disease extinction (when $\mathcal{R}_0 < 1$) or persistence (when
 75 $\mathcal{R}_0 > 1$), and gives guidance for disease control strategies.

76 First, we consider a toy model of a 4-node path graph network with counter-
 77 intuitive numerical results showing opposite monotonicity of \mathcal{R}_0 corresponding to a
 78 bypass from upstream to downstream (e.g., due to flooding). As depicted in Figure 1,
 79 we consider the spread of a pathogen (e.g., cholera) on a path network of 4 patches
 80 (vertices) with vertices 1, 2, 3, 4 sequentially located along a river, where vertex 1
 81 is upstream and vertex 4 is downstream. We assume that each nonzero movement
 82 rate, m_{ij} from vertex j to vertex i , on the path has value 1. As shown in [17, 44]
 83 the associated next generation matrix takes the form $K = FV^{-1} = D_q G_W^{-1} D_r G_I^{-1}$,
 84 where F is the matrix of new infections, V is the matrix of transitions, $D_q = \text{diag}\{q_i\}$,
 85 $G_W = \text{diag}\{\delta_i\} + L$, $D_r = \text{diag}\{r_i\}$ and $G_I = \text{diag}\{\mu_i\}$. Here the parameters q_i , δ_i , r_i
 86 and μ_i are the linearized indirect transmission rate (from pathogen to host), pathogen

87 decay rate, pathogen shedding rate and decay rate of infectious host individuals in
 88 patch i , respectively, ($i = 1, 2, 3, 4$). The matrix L is the 4×4 Laplacian matrix
 89 associated with M , i.e., $L = \text{diag}\{\sum_{j \neq i} m_{ji}\} - M$, where $M = (m_{ij})$ with $m_{ij} \geq 0$
 90 representing the pathogen/host dispersal from patch j to patch i . Then the exact
 91 network basic reproduction number is $\mathcal{R}_0 = \rho(FV^{-1}) = \rho(D_q G_W^{-1} D_r G_I^{-1})$, where ρ
 92 denotes the spectral radius. For simplicity, we set $r_i/\mu_i = 1, \delta_i = 1$ in each patch,
 93 with the base q_i value taken to be $q = 0.195$. In this case, the basic reproduction
 94 number in patch i is equal to q_i . We consider two scenarios in which the network
 95 has a ‘‘hot spot’’, i.e. a vertex i at which the linearized indirect transmission rate
 96 q_i (or equivalently $\mathcal{R}_0^{(i)}$) is higher than those of the other vertices, and an arc that
 97 bypasses the hot spot. In the first case (see the left plot in Figure 1), the hot spot
 98 is assumed to be located at vertex 2 with an additional bypass downstream from
 99 vertex 1 to vertex 3 being included, specifically, $q_1 = q_3 = q_4 = q, q_2 = 10q$, and

100
$$L = \begin{pmatrix} 1 + m_{31} & -1 & 0 & 0 \\ -1 & 2 & -1 & 0 \\ -m_{31} & -1 & 2 & -1 \\ 0 & 0 & -1 & 1 \end{pmatrix}$$
. In the second case (see the right plot in Figure 1),

101 the hot spot is located at vertex 3 and a new bypass from vertex 2 to vertex 4 is
 102 included with $q_1 = q_2 = q_4 = q, q_3 = 10q$ and
$$L = \begin{pmatrix} 1 & -1 & 0 & 0 \\ -1 & 2 + m_{42} & -1 & 0 \\ 0 & -1 & 2 & -1 \\ 0 & -m_{42} & -1 & 1 \end{pmatrix}$$
.

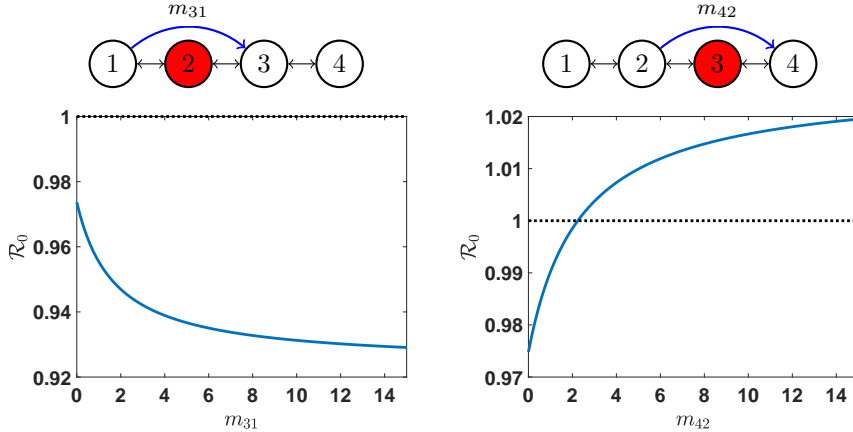


FIG. 1. With the hot spot at 2, \mathcal{R}_0 decreases as m_{31} increases (left plot); with the hot spot at 3, \mathcal{R}_0 increases as m_{42} increases (right plot).

103 In both cases the hot spot is bypassed, in the same direction, but the effects on
 104 \mathcal{R}_0 are markedly different, as shown in Figure 1. This unexpected behavior motivates
 105 our investigation of the effect of network structure on \mathcal{R}_0 .

106 The remainder of the article is organized as follows. Some preliminary results are
 107 provided in section 2. Two different methods, one combinatorial and one algebraic,
 108 are employed to investigate the impact of varying community networks on disease
 109 invasion, in sections 3 and 4, respectively. Applications to specific networks are il-
 110 lustrated in section 5, including an explanation of the counter-intuitive numerical
 111 results above. Disease control strategies involving varying the community network
 112 are considered in section 6, and concluding remarks are given in section 7.

113 **2. Preliminaries.** From consideration of a system of ordinary differential equa-
 114 tions governing the dynamics of cholera under the assumptions that humans become
 115 infected through contact with pathogens in the water, and that the water movement
 116 is faster than the pathogen decay rate, it has been established [17, 44] that \mathcal{R}_0 is
 117 approximated (from the exact value, given by the spectral radius of the next gen-
 118 eration matrix) by a linear combination of the basic reproduction numbers in each
 119 patch in isolation. The constants in this linear combination are the components of
 120 the normalized right eigenvector of the Laplacian matrix of the community network.
 121 The specific aim of this work is to determine how this eigenvector and \mathcal{R}_0 change with
 122 alterations in the network structure. We consider a strongly connected network, and
 123 assume that the network maintains this property when changed.

124 To be more precise, let $M = (m_{ij}) \geq 0$ denote an $n \times n$ irreducible matrix rep-
 125 resenting the pathogen/host movement in a heterogeneous environment of n patches.
 126 In particular, when $1 \leq i, j \leq n$ are distinct, $m_{ij} \geq 0$ represents the pathogen/host
 127 dispersal from patch j to patch i . We assume that $m_{ii} = 0$ for $i = 1, \dots, n$. Let
 128 $\mathcal{G} = \mathcal{G}(M)$ be the weighted digraph associated with M . That is, in \mathcal{G} there is an arc
 129 $j \rightarrow i$ from vertex j to vertex i of weight m_{ij} if and only if $m_{ij} > 0$. Let L be the
 130 Laplacian matrix of $\mathcal{G}(M)$, i.e.,

$$131 \quad (2.1) \quad L = \text{diag} \left(\sum_{i \neq 1} m_{i1}, \sum_{i \neq 2} m_{i2}, \dots, \sum_{i \neq n} m_{in} \right) - M.$$

132 Notice that each column sum of L is 0, and thus 0 is an algebraically simple eigenvalue
 133 of L (since M is irreducible). Evidently the all ones vector, $\mathbb{1}^\top$, is a left null vector for
 134 L . For each $k = 1, \dots, n$, let $C_{kk} = \det(L_{(k,k)})$ be the principal minor of L formed by
 135 deleting its k -th row and column. Consider the vector $u = (u_1, u_2, \dots, u_n)^\top$, where

$$136 \quad (2.2) \quad u_k = \frac{C_{kk}}{\sum_{\ell=1}^n C_{\ell\ell}}, \quad k = 1, \dots, n.$$

137 Denote the adjugate of L by $\text{adj}(L)$, and recall that $L \text{adj}(L) = \text{adj}(L)L = \det(L)I =$
 138 0 . Hence $\text{adj}(L) = x \mathbb{1}^\top$, where x is a nonzero vector in the right null space of L . It
 139 now follows that u is the right null vector of L , normalized so that $\mathbb{1}^\top u = 1$.

140 As shown in [17, 44] (also see [8]), when the time scale of movement is substan-
 141 tially larger than the time scale of the disease dynamics, the coefficients u_k defined
 142 above serve as weights to aggregate the disease dynamics from each patch. For this
 143 reason, u_k is called the *network risk* of patch k . In particular, the network basic re-
 144 production number \mathcal{R}_0 can be approximated by the u -weighted average of the patch
 145 basic reproduction numbers $\mathcal{R}_0^{(k)}$; that is,

$$146 \quad (2.3) \quad \mathcal{R}_0 \approx \sum_{k=1}^n u_k \mathcal{R}_0^{(k)}.$$

147 This expression (2.3) separates the structure of the movement network and the
 148 within-patch disease dynamics, and thus provides a new approach to investigate the
 149 impact of changes in the network on disease invasion. Specifically, we first investigate
 150 how a change to the network structure affects the network risks u_k , and then utilize
 151 the aggregation in (2.3) to understand how varying the network affects the disease
 152 invasibility (i.e., the value of \mathcal{R}_0).

153 Since u_k depends on the cofactor C_{kk} as in (2.2), it can be expressed in terms
 154 of the sum of weights of spanning rooted trees [11, 36] by using Kirchhoff's Matrix-
 155 Tree Theorem. Calculating the weights of such trees gives a combinatorial method

156 for finding the sign of $\frac{du_k}{dm_{ij}}$, the derivative of u_k with respect to a change in the arc
 157 $j \rightarrow i$. This combinatorial approach is developed in section 3, and may be convenient
 158 for some cases, such as small networks or networks with specific structures.

159 In addition, there is a well-established algebraic tool for understanding how
 160 changes in the movement matrix M affect the entries in the right null vector u of the
 161 Laplacian matrix L . Since L is a singular and irreducible M-matrix, the eigenvalue 0
 162 of L is algebraically simple; so, while L is not invertible, it has a *group inverse*, that
 163 is, a unique matrix $L^\#$ such that $LL^\# = L^\#L$, $LL^\#L = L$, and $L^\#LL^\# = L^\#$. The
 164 group inverse has been used effectively to analyse how changes in an irreducible non-
 165 negative matrix affect its Perron eigenvalue and eigenvector (see for example [14, 34])
 166 and our results in section 4 are informed by that approach. We refer the interested
 167 reader to [7] for background on generalized inverses in general, and to [28] for the use
 168 of the group inverses in the study of M-matrices in particular.

169 With the group inverse method developed in generality, in section 5.1, we illustrate
 170 this method with a star network in which one patch is the hub connected to several leaf
 171 vertices. Such a network structure is appropriate as a model for a large city connected
 172 to smaller cities or suburbs, with humans commuting in each direction. Then in
 173 section 5.2, we illustrate the general results for a path network, which models cholera
 174 outbreaks in communities living along a river. For these two network structures, we
 175 consider control strategies for restricted cases of the two networks (section 6), and
 176 derive results on how changes to the network can help to minimize disease invasion.

177 **3. Combinatorial method: counting spanning rooted trees.** It follows
 178 from Kirchhoff’s Matrix–Tree Theorem [11, 36] that the cofactor of the (k, k) entry
 179 of L can be interpreted in terms of spanning rooted trees:

180 (3.1)
$$C_{kk} = \sum_{\mathcal{T} \in \mathbb{T}_k} w(\mathcal{T}) =: W_k,$$

181 where \mathbb{T}_k is the set of spanning in-trees rooted at vertex k and $w(\mathcal{T}) = \prod_{(j,i) \in E(\mathcal{T})} m_{ij}$
 182 is the weight of a spanning in-tree \mathcal{T} rooted at k . The notation W_k introduced in
 183 (3.1) is convenient for tracking how $u_k = \frac{W_k}{\sum_\ell W_\ell}$, defined in (2.2), behaves as the
 184 network structure changes. Specifically, we consider a small change of the m_{ij} value
 185 (for a fixed ordered pair (i, j)) in the movement network, say $m_{ij} \rightarrow m_{ij} + \epsilon$, and
 186 explore how the value of u_k responds; to do so, we focus on the sign of $\frac{du_k}{dm_{ij}}$. (We
 187 note in passing that if m_{ij} is zero, we only consider positive values of ϵ , and in that
 188 setting $\frac{du_k}{dm_{ij}}$ is interpreted as the derivative from the right.) Notice that such a change
 189 $m_{ij} \rightarrow m_{ij} + \epsilon$ affects two entries of L ; the (i, j) entry and the (j, j) entry.

190 Before establishing our main results, we introduce some additional notation and
 191 tools from matrix theory and graph theory. Let $L_{(ij,kl)}$ denote the matrix obtained
 192 from L by deleting the i -th and j -th rows and k -th and ℓ -th columns. Let W_k^{ij}
 193 denote the sum of the weights of all spanning in-trees rooted at k containing the arc
 194 $j \rightarrow i$, and let $W_k^{\sim ij}$ denote the sum of the weights of all spanning in-trees rooted at
 195 k that do not contain the arc $j \rightarrow i$. Notice that $W_k = W_k^{ij} + W_k^{\sim ij}$.

196 First we prove the following two lemmas.

197 LEMMA 3.1. *Assume $i \neq j$. Then*

198 (3.2)
$$W_k^{ij} = m_{ij} |\det(L_{(ij,kj)})|.$$

199 *Proof.* From the all-minors Matrix–Tree Theorem [11], $|\det(L_{(ij,kj)})|$ is the sum
 200 of the weights of all spanning forests \mathcal{F} that contain exactly two in-tree components,

201 one rooted at k containing vertex i and the other rooted at j . Adding the arc $j \rightarrow$
 202 i of weight m_{ij} in \mathcal{F} , yields a spanning in-tree \mathcal{T} rooted at k containing $j \rightarrow i$;
 203 in particular, $m_{ij}w(\mathcal{F}) = w(\mathcal{T})$. The identity (3.2) follows after performing this
 204 operation for all spanning forests. \square

205 We note here that strictly speaking, the right side of (3.2) is not defined in the
 206 case that $k = j$. However, we may adopt the convention that $\det(L_{(ij,kk)}) = 0$, and
 207 then (3.2) will also hold when $k = j$.

208 LEMMA 3.2. *Let $W_k = C_{kk} = \det(L_{(k,k)})$. Then, for any $i \neq j$,*

$$209 \quad (3.3) \quad \frac{dW_k}{dm_{ij}} = |\det(L_{(ij,kj)})|.$$

210 *Proof.* Straightforward calculations, along with (3.2), yield

$$\begin{aligned} 211 \quad \frac{dW_k}{dm_{ij}} &= \lim_{\epsilon \rightarrow 0} \frac{(W_k^{ij} + W_k^{\sim ij})|_{m_{ij}+\epsilon} - (W_k^{ij} + W_k^{\sim ij})|_{m_{ij}}}{\epsilon} \\ 212 \quad &= \lim_{\epsilon \rightarrow 0} \frac{(m_{ij} + \epsilon)|\det(L_{(ij,kj)})| + W_k^{\sim ij} - m_{ij}|\det(L_{(ij,kj)})| - W_k^{\sim ij}}{\epsilon} \\ 213 \quad &= |\det(L_{(ij,kj)})|, \end{aligned}$$

215 resulting in (3.3). \square

216 As with (3.2), when $k = j$, we interpret both sides of (3.3) as being zero.

217 In particular, if $m_{ij} > 0$ for $i \neq j$, it follows from Lemmas 3.1 and 3.2 that

$$218 \quad (3.4) \quad \frac{dW_k}{dm_{ij}} = \frac{W_k^{ij}}{m_{ij}}.$$

220 Now we are ready to prove the main result arising from this combinatorial method.

221 THEOREM 3.3. *For any given $k, i, j, i \neq j$,*

$$222 \quad (3.5) \quad \operatorname{sgn}\left(\frac{du_k}{dm_{ij}}\right) = \operatorname{sgn}\left(|\det(L_{(ij,kj)})| \sum_{\ell \neq k} W_\ell - W_k \sum_{\ell \neq k} |\det(L_{(ij,\ell j)})|\right).$$

223 *If, in addition, $m_{ij} > 0$, then*

$$224 \quad (3.6) \quad \operatorname{sgn}\left(\frac{du_k}{dm_{ij}}\right) = \operatorname{sgn}\left(W_k^{ij} \sum_{\ell \neq k} W_\ell^{\sim ij} - W_k^{\sim ij} \sum_{\ell \neq k} W_\ell^{ij}\right).$$

225 *Proof.* Taking the derivative on both sides of (2.2) with respect to m_{ij} yields

$$226 \quad (3.7) \quad \frac{du_k}{dm_{ij}} = \frac{1}{(\sum_\ell W_\ell)^2} \left(\frac{dW_k}{dm_{ij}} \sum_\ell W_\ell - W_k \sum_\ell \frac{dW_\ell}{dm_{ij}} \right).$$

227 Substituting (3.3) into (3.7), after the cancellation of the case $\ell = k$, yields (3.5).

228 Additionally, if $m_{ij} > 0$, then it follows from (3.4) that

$$229 \quad (3.8) \quad \frac{du_k}{dm_{ij}} = \frac{1}{(\sum_\ell W_\ell)^2} \left(\frac{W_k^{ij}}{m_{ij}} \sum_{\ell \neq k} W_\ell - W_k \sum_{\ell \neq k} \frac{W_\ell^{ij}}{m_{ij}} \right)$$

$$230 \quad (3.9) \quad = \frac{1}{m_{ij}(\sum_\ell W_\ell)^2} \left(W_k^{ij} \sum_{\ell \neq k} (W_\ell^{ij} + W_\ell^{\sim ij}) - (W_k^{ij} + W_k^{\sim ij}) \sum_{\ell \neq k} W_\ell^{ij} \right)$$

$$231 \quad (3.10) \quad = \frac{1}{m_{ij}(\sum_\ell W_\ell)^2} \left(W_k^{ij} \sum_{\ell \neq k} W_\ell^{\sim ij} - W_k^{\sim ij} \sum_{\ell \neq k} W_\ell^{ij} \right),$$

232

233 resulting in (3.6). \square

234 The sign identities (3.5) and (3.6) characterize how the network risk at patch k
 235 changes as a function of the movement from patch j to patch i . If more information
 236 on the movement network is provided, the exact sign of $\frac{du_k}{dm_{ij}}$ may be able to be
 237 determined. If patch k is the head of the altered arc $j \rightarrow i$ (i.e., $j = k$), then the sign
 238 of the change in the network risk $\frac{du_k}{dm_{ij}}$ is determined in the following result, regardless
 239 of the network structure.

240 **THEOREM 3.4.** *For any given $k, i, i \neq k$, $\frac{du_k}{dm_{ik}} < 0$.*

241 *Proof.* Since there is no spanning in-tree rooted at k that contains the arc $k \rightarrow i$
 242 (i.e., leaving the root vertex k), $W_k^{ij} = 0$. It follows from the irreducibility of M that
 243 there exists at least one spanning in-tree rooted at k , which certainly does not contain
 244 the arc $k \rightarrow i$; thus $W_k^{\sim ik} > 0$. If $m_{ik} > 0$, then there exists at least one vertex $\ell \neq k$
 245 at which a spanning in-tree containing $k \rightarrow i$ is rooted, and hence $W_\ell^{ik} > 0$. It follows
 246 from (3.6) that $\frac{du_k}{dm_{ik}} < 0$.

247 If $m_{ik} = 0$, then (3.5) can be utilized to establish the result. Specifically, there
 248 is no spanning forest of two components both of which are rooted at k , which is
 249 reflected in our convention that $\det(L_{(ij,kk)}) = 0$. Similarly, the irreducibility of M
 250 implies that $W_k > 0$ and $|\det(L_{(ij,\ell k)})| > 0$ for some $\ell \neq k$. \square

251 Notice that none of the in-trees rooted at k include the arc $k \rightarrow i$, so any increase
 252 of m_{ik} does not alter W_k but increases all other $W_\ell, \ell \neq k$. Consequently, all terms
 253 in the first sum of (3.5) or (3.6) vanish, as shown in the proof of Theorem 3.4. In
 254 contrast, perturbations of m_{kj} change W_k and other $W_\ell, \ell \neq k$, which requires more
 255 discussion.

256 If patch k is the tail of the altered arc $j \rightarrow i$ (i.e., $k = i$), and the restriction is
 257 added that the only path from j to k is the arc $j \rightarrow k$, then the proof of the following
 258 result proceeds by an analysis similar to that used to prove Theorem 3.4.

259 **THEOREM 3.5.** *For any given $k, j, j \neq k$, if the arc $j \rightarrow k$ is the only path from*
 260 *j to k , then $W_k^{\sim kj} = 0$, and $\frac{du_k}{dm_{kj}} > 0$.*

261 In section 4, we generalize Theorem 3.5 by using the group inverse to remove the
 262 restriction on the number of paths from j to k .

263 **4. Algebraic method: computing the group inverse.** Suppose that L is an
 264 irreducible Laplacian matrix with zero column sums, as in (2.1). Recall from section
 265 2 that there is a unique group inverse $L^\#$ such that $LL^\# = L^\#L, LL^\#L = L$, and
 266 $L^\#LL^\# = L^\#$. The left and right null spaces of L are necessarily one-dimensional,
 267 and are spanned by $\mathbb{1}^\top$ and u , respectively, where $u = (u_1, \dots, u_n)^\top$ is the right null
 268 vector of L , normalized so that $\mathbb{1}^\top u = \sum_{i=1}^n u_i = 1$. From Corollary 7.2.1 of [7], it
 269 now follows that $L^\#L = I - u\mathbb{1}^\top$.

270 Consider a perturbation $\tilde{L} = L + E$ of L such that \tilde{L} is also a singular and
 271 irreducible M-matrix with $\mathbb{1}^\top \tilde{L} = 0$. We seek the normalized right null vector of \tilde{L} ;
 272 i.e., the vector \tilde{u} such that $\tilde{L}\tilde{u} = 0$ and $\mathbb{1}^\top \tilde{u} = 1$. Since $(L + E)\tilde{u} = 0$, we have
 273 $L^\#(L + E)\tilde{u} = 0$, and hence $(I - u\mathbb{1}^\top)\tilde{u} + L^\#E\tilde{u} = 0$. Thus $(I + L^\#E)\tilde{u} = u$. Since
 274 $I + L^\#E$ is invertible (see [34], or Lemma 5.3.1 in [28]), this gives

$$275 \quad (4.1) \quad \tilde{u} = (I + L^\#E)^{-1}u.$$

276 At the end of this section, we provide an explicit expression for $L^\#$.

277 The following technical result is useful in proving Theorem 4.2 below.

278 LEMMA 4.1 ([24, 35]). Let x and y be column vectors of dimension n . If $y^\top x \neq$
 279 -1 , then $(I + xy^\top)^{-1} = I - \frac{1}{1+y^\top x}xy^\top$.

280 Here is one of the main results in this section.

281 THEOREM 4.2. Let L be an irreducible M -matrix as defined in (2.1).

282 a) Suppose that $L + \epsilon F$ is an irreducible M -matrix with $\mathbb{1}^\top F = 0$ for all ϵ in a
 283 neighborhood of 0. Then the directional derivative of u with respect to F is $-L^\# F u$.

284 b) Perturb $m_{ij} \rightarrow m_{ij} + \epsilon$ (where $\epsilon \geq 0$ when $m_{ij} = 0$) with $1 \leq i \neq j \leq n$, and denote
 285 the corresponding right null vector for the Laplacian (normalized to have sum 1) by
 286 \tilde{u} . Then for $k = 1, \dots, n$,

$$287 \quad (4.2) \quad \tilde{u}_k - u_k = -\frac{\epsilon u_j e_k^\top L^\#(e_j - e_i)}{1 + \epsilon e_j^\top L^\#(e_j - e_i)} = -\frac{\epsilon u_j (L_{kj}^\# - L_{ki}^\#)}{1 + \epsilon (L_{jj}^\# - L_{ji}^\#)}.$$

288 Moreover,

$$289 \quad (4.3) \quad \frac{du_k}{dm_{ij}} = -u_j e_k^\top L^\#(e_j - e_i) = -u_j (L_{kj}^\# - L_{ki}^\#), \quad k = 1, \dots, n,$$

$$290 \quad \text{and } \frac{1}{u_j} \frac{du_k}{dm_{ij}} = -\frac{1}{u_i} \frac{du_k}{dm_{ji}}, \quad k = 1, \dots, n.$$

291 *Proof.* a) For ϵ sufficiently small,

$$292 \quad (4.4) \quad (I + \epsilon L^\# F)^{-1} = I - \epsilon L^\# F + O(\epsilon^2).$$

293 Taking $E = \epsilon F$ in (4.1) and using (4.4) yields

$$294 \quad (4.5) \quad \tilde{u} = (I + L^\# E)^{-1} u = (I - \epsilon L^\# F) u + O(\epsilon^2) = u - \epsilon L^\# F u + O(\epsilon^2).$$

295 Hence $\lim_{\epsilon \rightarrow 0} \frac{\tilde{u} - u}{\epsilon} = -L^\# F u$, as desired.

296

297 b) Set $E = \epsilon(-e_i + e_j)e_j^\top$. From (4.1), it follows that $\tilde{u} = (I + L^\# E)^{-1} u$, and
 298 Lemma 4.1 gives $(I + L^\# E)^{-1} = I - \frac{\epsilon}{1 + \epsilon e_j^\top L^\#(-e_i + e_j)} L^\#(-e_i + e_j)e_j^\top$. (Observe that
 299 since $I + \epsilon L^\#(-e_i + e_j)e_j^\top$ is invertible, $1 + \epsilon e_j^\top L^\#(-e_i + e_j) = \det(I + \epsilon L^\#(-e_i +$
 300 $e_j)e_j^\top) \neq 0$.) The conclusions now follow readily. \square

301 Next we discuss how to find $L^\#$. From the hypotheses on L , it is easy to see that
 302 L may be partitioned as

$$303 \quad L = \left(\begin{array}{c|c} \bar{\mathbb{1}}^\top z & -\bar{\mathbb{1}}^\top B \\ \hline -z & B \end{array} \right)$$

304 where B is an $(n-1) \times (n-1)$ invertible matrix, u_1 is the first entry of u , $\bar{u} =$
 305 $(u_2, \dots, u_n)^\top$, $z = \frac{1}{u_1} B \bar{u}$, and $\bar{\mathbb{1}}$ is the all ones column vector of dimension $n-1$.

306 It follows from Observation 2.3.4 of [28] that

$$307 \quad (4.6) \quad L^\# = (\bar{\mathbb{1}}^\top B^{-1} \bar{u}) u \mathbb{1}^\top + \left(\begin{array}{c|c} 0 & -u_1 \bar{\mathbb{1}}^\top B^{-1} \\ \hline -B^{-1} \bar{u} & B^{-1} - B^{-1} \bar{u} \bar{\mathbb{1}}^\top - \bar{u} \bar{\mathbb{1}}^\top B^{-1} \end{array} \right).$$

308 Suppose that $1 \leq i < j \leq n$; partitioning out the first entry as above gives

$$309 \quad (4.7) \quad L^\#(e_j - e_i) = \begin{cases} \left(\begin{array}{c} -u_1 \bar{\mathbb{1}}^\top B^{-1} e_{j-1} \\ B^{-1} e_{j-1} - \bar{u} \bar{\mathbb{1}}^\top B^{-1} e_{j-1} \end{array} \right), & \text{if } i = 1, \\ \left(\begin{array}{c} -u_1 \bar{\mathbb{1}}^\top B^{-1} (e_{j-1} - e_{i-1}) \\ B^{-1} (e_{j-1} - e_{i-1}) - \bar{u} \bar{\mathbb{1}}^\top B^{-1} (e_{j-1} - e_{i-1}) \end{array} \right), & \text{if } 2 \leq i \leq n. \end{cases}$$

310 From (4.7), we find that $e_1^\top L^\#(e_1 - e_j) > 0, j = 2, \dots, n$. The rows and columns of L
 311 can be simultaneously permuted to place any index in the first position, and hence

$$312 \quad (4.8) \quad L_{jj}^\# - L_{ji}^\# > 0, \quad i, j = 1, \dots, n, \quad i \neq j.$$

313 Suppose that $1 \leq i < j \leq n$. If we perturb $m_{ij} \rightarrow m_{ij} + \epsilon$ (where $\epsilon \geq 0$ when
 314 $m_{ij} = 0$), it follows from (4.2) and (4.7) that

$$315 \quad \tilde{u}_1 - u_1 = \begin{cases} \frac{\epsilon u_1 u_j \bar{\mathbb{1}}^\top B^{-1} e_{j-1}}{1 + \epsilon e_{j-1}^\top (B^{-1} e_{j-1} - \bar{u} \bar{\mathbb{1}}^\top B^{-1} e_{j-1})}, & i = 1, \\ \frac{\epsilon u_1 u_j \bar{\mathbb{1}}^\top B^{-1} (e_{j-1} - e_{i-1})}{1 + \epsilon e_{j-1}^\top [B^{-1} (e_{j-1} - e_{i-1}) - \bar{u} \bar{\mathbb{1}}^\top B^{-1} (e_{j-1} - e_{i-1})]}, & 2 \leq i \leq n. \end{cases}$$

316 For $2 \leq \ell \leq n$, we have

$$317 \quad \tilde{u}_\ell - u_\ell = \begin{cases} -\frac{\epsilon u_j e_{\ell-1}^\top (B^{-1} e_{j-1} - \bar{u} \bar{\mathbb{1}}^\top B^{-1} e_{j-1})}{1 + \epsilon e_{j-1}^\top (B^{-1} e_{j-1} - \bar{u} \bar{\mathbb{1}}^\top B^{-1} e_{j-1})}, & i = 1, \\ -\frac{\epsilon u_j e_{\ell-1}^\top [B^{-1} (e_{j-1} - e_{i-1}) - \bar{u} \bar{\mathbb{1}}^\top B^{-1} (e_{j-1} - e_{i-1})]}{1 + \epsilon e_{j-1}^\top [B^{-1} (e_{j-1} - e_{i-1}) - \bar{u} \bar{\mathbb{1}}^\top B^{-1} (e_{j-1} - e_{i-1})]}, & 2 \leq i \leq n. \end{cases}$$

318 *Remark 4.1.* By considering (4.3) and (4.8) for the cases $j = k$ and $i = k$, we
 319 find an alternate proof for Theorem 3.4, and an extension of Theorem 3.5 that goes
 320 through without the path restriction.

321 **5. Applications to specific networks.** In this section, we apply our general
 322 results to two different networks: a star network for human transportation between
 323 one hub and several leaves, and a path network for communities along a river.

324 **5.1. Star network.** First, we consider a star network with vertex 1 as the hub,
 325 and $2, 3, \dots, n$ as leaf vertices, with corresponding weights $m_{1j}, m_{j1} > 0, j = 2, \dots, n$.
 326 Assuming that a new arc from leaf $j > 1$ to leaf $i > 1$ is added, the following result
 327 shows that the direction of change of the network risk u_k at any other vertex (i.e.,
 328 $k \neq i, k \neq j$) depends only on m_{1i} and m_{1j} .

329 **THEOREM 5.1.** *For a star network, let i, j be any two distinct leaf vertices and k
 330 be another vertex. Then $\text{sgn} \left(\frac{du_k}{dm_{ij}} \right) = \text{sgn}(m_{1i} - m_{1j})$.*

331 To illustrate both combinatorial and algebraic methods in sections 3 and 4, we
 332 prove the above result using two different approaches.

333 Combinatorial Proof of Theorem 5.1: By Theorem 3.3, it suffices to determine the
 334 sign of

$$335 \quad (5.1) \quad W_k^{ij} \sum_{\ell \neq k} W_\ell^{\sim ij} - W_k^{\sim ij} \sum_{\ell \neq k} W_\ell^{ij},$$

336 which involves the weights of certain specific spanning rooted trees. As depicted in
 337 Figure 2, $W_k^{ij} = m_{k1} m_{1i} m_{ij} \prod_s m_{1s}$ and $W_k^{\sim ij} = m_{k1} m_{1i} m_{1j} \prod_s m_{1s}$, where s takes
 338 all values except $1, k, i, j$, corresponding to the unique spanning in-tree rooted at k
 339 that contains the arc $j \rightarrow i$ and does not contain the arc $j \rightarrow i$, respectively. Now
 340 we consider spanning in-trees rooted at $\ell \neq k$, containing $j \rightarrow i$ or not, which con-
 341 tributes terms appearing in the sums of (5.1). Specifically, we consider three cases:
 342 $\ell = i, \ell = j$, and all other possible values (i.e., $\ell = r$, where $r \neq k, i, j$). As de-
 343 picted in Figure 2, $W_i^{\sim ij} = m_{i1} m_{1j} m_{1k} \prod_s m_{1s}$, $W_j^{\sim ij} = m_{j1} m_{1i} m_{1k} \prod_s m_{1s}$, $W_r^{\sim ij} =$

344 $m_{r1}m_{1i}m_{1j}m_{1k} \prod_s m_{1s}/m_{1r}$; $W_i^{ij} = m_{i1}m_{ij}m_{1k} \prod_s m_{1s} + m_{ij}m_{j1}m_{1k} \prod_s m_{1s}$,
 345 $W_j^{ij} = 0$, $W_r^{ij} = m_{r1}m_{1i}m_{ij}m_{1k} \prod_s m_{1s}/m_{1r}$. Here s takes all values except $1, k, i, j$,
 346 and notice that there are two spanning in-trees rooted at i containing $j \rightarrow i$ while no
 347 spanning in-tree rooted at j contains $j \rightarrow i$. There is immediate cancellation in (5.1)
 348 since $W_k^{ij}W_r^{\sim ij} = W_k^{\sim ij}W_r^{ij}$, for all r . After simplification, (5.1) becomes

$$\begin{aligned}
 349 \quad & W_k^{ij} \sum_{\ell \neq k} W_\ell^{\sim ij} - W_k^{\sim ij} \sum_{\ell \neq k} W_\ell^{ij} = W_k^{ij} [W_i^{\sim ij} + W_j^{\sim ij}] - W_k^{\sim ij} [W_i^{ij} + W_j^{ij}] \\
 350 \quad & = m_{k1}m_{1i}m_{ij} \prod_s m_{1s} \left[m_{i1}m_{1j}m_{1k} \prod_s m_{1s} + m_{j1}m_{1i}m_{1k} \prod_s m_{1s} \right] \\
 351 \quad & \quad - m_{k1}m_{1i}m_{1j} \prod_s m_{1s} \left[m_{i1}m_{ij}m_{1k} \prod_s m_{1s} + m_{ij}m_{j1}m_{1k} \prod_s m_{1s} \right] \\
 352 \quad & = m_{k1}m_{1i}m_{j1}m_{1k}m_{ij} \left(\prod_s m_{1s} \right)^2 (m_{1i} - m_{1j}), \\
 353 \quad & \\
 354 \quad & \text{completing the proof.} \quad \square
 \end{aligned}$$

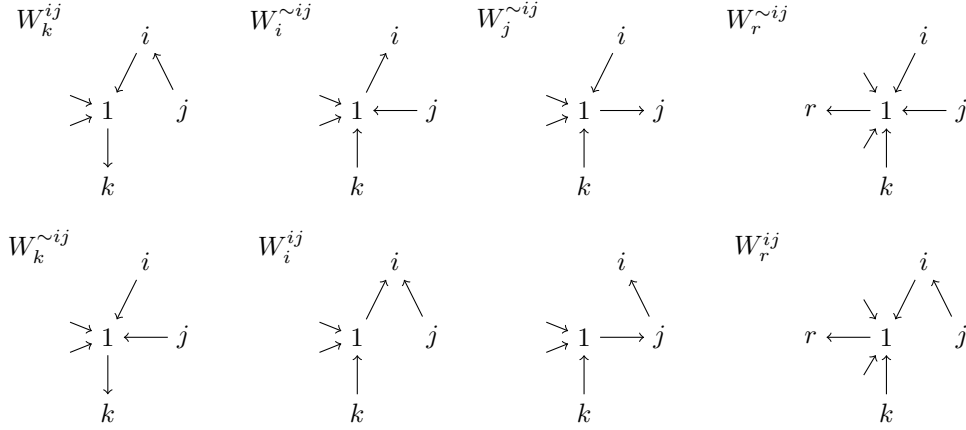


FIG. 2. Spanning rooted trees with certain specific restrictions in a star network (1 is the hub). Notice that there is no spanning in-tree rooted at j that contains the arc $j \rightarrow i$, so $W_j^{ij} = 0$.

355 Algebraic Proof of Theorem 5.1: Consider a star network with vertex 1 as the hub,
 356 and $2, 3, \dots, n$ as leaf vertices. From the hypothesis,

$$357 \quad (5.2) \quad L = \begin{pmatrix} \sum_{i \neq 1} m_{i1} & -m_{12} & -m_{13} & \dots & -m_{1n} \\ -m_{21} & m_{12} & 0 & \dots & 0 \\ -m_{31} & 0 & m_{13} & \dots & 0 \\ \vdots & \vdots & \vdots & \ddots & \vdots \\ -m_{n1} & 0 & 0 & \dots & m_{1n} \end{pmatrix}$$

358 For concreteness, consider $i = 2$ and $j = 3$. It follows from (4.3) that

$$359 \quad (5.3) \quad \frac{du}{dm_{23}} = -u_3 L^\#(-e_2 + e_3).$$

360 To determine the sign of $\frac{du}{dm_{23}}$, we need to compute the right hand side of (5.3).

361 As $u_3 > 0$, $\text{sgn}\left(\frac{du}{dm_{23}}\right) = \text{sgn}(-L^\#(-e_2 + e_3))$. Since $B = \text{diag}(m_{12}, \dots, m_{1n})$ is

362 diagonal, $u_1 \bar{1}^\top B^{-1}(-e_1 + e_2) = u_1 \left(-\frac{1}{m_{12}} + \frac{1}{m_{13}}\right)$, which implies that

$$(B^{-1} - \bar{u}\bar{1}^\top B^{-1})(-e_1 + e_2) = \begin{pmatrix} -\frac{1}{m_{12}} \\ \frac{1}{m_{13}} \\ 0 \\ \vdots \\ 0 \end{pmatrix} - \begin{pmatrix} u_2 \\ u_3 \\ u_4 \\ \vdots \\ u_n \end{pmatrix} \left(-\frac{1}{m_{12}} + \frac{1}{m_{13}} \right).$$

So

$$-L^\#(-e_2 + e_3) = - \begin{pmatrix} -u_1 \left(-\frac{1}{m_{12}} + \frac{1}{m_{13}} \right) \\ \left(-\frac{1}{m_{12}} \right) \\ \left(\frac{1}{m_{13}} \right) \\ 0 \\ \vdots \\ 0 \end{pmatrix} - \begin{pmatrix} u_2 \\ u_3 \\ u_4 \\ \vdots \\ u_n \end{pmatrix} \left(-\frac{1}{m_{12}} + \frac{1}{m_{13}} \right).$$

Thus,

$$\text{sgn}(\tilde{u}_1 - u_1) = \text{sgn}(m_{12} - m_{13}),$$

$$\text{sgn}(\tilde{u}_2 - u_2) = -\text{sgn}\left(\frac{-m_{13} - u_2(m_{12} - m_{13})}{m_{12}m_{13}}\right) = \text{sgn}(m_{13} + u_2(m_{12} - m_{13})),$$

$$\text{sgn}(\tilde{u}_3 - u_3) = -\text{sgn}\left(\frac{m_{12} - u_3(m_{12} - m_{13})}{m_{12}m_{13}}\right) = \text{sgn}(-m_{12} + u_3(m_{12} - m_{13})),$$

$$\text{sgn}(\tilde{u}_\ell - u_\ell) = \text{sgn}\left(\frac{u_\ell(m_{12} - m_{13})}{m_{12}m_{13}}\right) = \text{sgn}(m_{12} - m_{13}), \ell = 4, \dots, n.$$

□

COROLLARY 5.2. For a star network with vertex 1 as the hub, the direction of change of the the network risk u_k is given by the following:

$$\begin{aligned} \text{sgn}\left(\frac{du_k}{dm_{ij}}\right) &= \text{sgn}(m_{1i} - m_{1j}), \quad k \neq i, j, i \neq 1, j \neq 1, \\ \text{sgn}\left(\frac{du_i}{dm_{ij}}\right) &> 0, \text{sgn}\left(\frac{du_j}{dm_{ij}}\right) < 0. \end{aligned}$$

5.2. River network. Consider a path network with vertices labeled $1, 2, 3, \dots, n$ consecutively located along a river, where 1 denotes the vertex that is farthest upstream and n is the vertex that is farthest downstream. Suppose further that the associated movement matrix M is constant along its superdiagonal and constant along its subdiagonal. (This corresponds to constant dispersal rates for upstream and downstream movement.) The corresponding Laplacian matrix \hat{L} is given by

$$\hat{L} = \begin{pmatrix} a & -b & 0 & \cdots & 0 & 0 \\ -a & a+b & -b & \cdots & 0 & 0 \\ 0 & -a & a+b & \cdots & 0 & 0 \\ \vdots & \vdots & & & & \\ 0 & 0 & 0 & \cdots & a+b & -b \\ 0 & 0 & 0 & \cdots & -a & b \end{pmatrix}$$

for $a > 0$ and $b > 0$. It suffices to consider the case that $a \geq b$; see the supplementary material for a justification. Henceforth we restrict to the case that $a \geq b$.

381 Setting $\alpha = \frac{a}{b}$ yields

$$382 \quad (5.6) \quad \hat{L} = b \begin{pmatrix} \alpha & -1 & 0 & \cdots & 0 & 0 \\ -\alpha & \alpha+1 & -1 & \cdots & 0 & 0 \\ 0 & -\alpha & \alpha+1 & \cdots & 0 & 0 \\ \vdots & \vdots & \vdots & \ddots & \vdots & \vdots \\ 0 & 0 & 0 & \cdots & \alpha+1 & -1 \\ 0 & 0 & 0 & \cdots & -\alpha & 1 \end{pmatrix} := bL.$$

383 Our assumption that $a \geq b$ gives $\alpha \geq 1$, and we note that this fits with our interpre-
384 tation of 1 being an upstream vertex and n being a downstream vertex. It is readily
385 verified that the vector $u = (u_1, u_2, \dots, u_n)^\top = \frac{1}{\sum_{\ell=0}^{n-1} \alpha^\ell} (1, \alpha, \alpha^2, \dots, \alpha^{n-1})^\top$ is the
386 right null vector of L normalized so that $\mathbb{1}^\top u = 1$. Let B denote the principal sub-
387 matrix of L formed by deleting the first row and column. A proof by induction on n
388 shows that the (k, j) entry of B^{-1} is given by

$$389 \quad e_k^\top B^{-1} e_j = \begin{cases} 1 + \alpha + \alpha^2 + \cdots + \alpha^{k-1}, & 1 \leq k \leq j \leq n-1, \\ \alpha^{k-j} (1 + \alpha + \alpha^2 + \cdots + \alpha^{j-1}), & 1 \leq j < k \leq n-1. \end{cases}$$

390 It can be shown by induction on n that the sum of the entries in column j of B^{-1} is

$$391 \quad \mathbb{1}^\top B^{-1} e_j = j \sum_{\ell=0}^{n-j-1} \alpha^\ell + \sum_{\ell=n-j}^{n-2} (n-1-\ell) \alpha^\ell, \quad j = 1, 2, \dots, n-1$$

392 where the empty sum is interpreted as zero.

393 The following is straightforward.

394 LEMMA 5.3. *Suppose that $m \geq 0$ and $n \in \mathbb{N}$. Then*

$$395 \quad \left(\sum_{\ell=0}^m \alpha^\ell \right) \left(\sum_{\ell=0}^{n-1} \alpha^\ell \right) = \sum_{\ell=0}^m (\ell+1) \alpha^\ell + (m+1) \sum_{\ell=m+1}^{n-1} \alpha^\ell + \sum_{\ell=n}^{n+m-1} (n+m-\ell) \alpha^\ell.$$

396 The following can be deduced from (4.7) and our expression for B^{-1} .

397 LEMMA 5.4. *For a path network, if $1 \leq i < j \leq n$, then*

$$398 \quad L_{jj}^\# - L_{ji}^\# = \frac{\sum_{\ell=0}^{j-i-1} (\ell+1) \alpha^\ell + (j-i) \sum_{\ell=j-i}^{j-2} \alpha^\ell}{\sum_{\ell=0}^{n-1} \alpha^\ell}.$$

399 Lemmas 5.3 and 5.4, along with (4.7) establish the following result.

400 THEOREM 5.5. *On a path network, if $1 \leq k \leq j \leq n$, then*

$$401 \quad e_k^\top L^\# (e_j - e_1) =$$

$$402 \quad \frac{1}{\sum_{\ell=0}^{n-1} \alpha^\ell} \left(\sum_{\ell=0}^{k-2} (\ell+1) \alpha^\ell - (j-k) \sum_{\ell=k-1}^{n+k-j-1} \alpha^\ell - \sum_{\ell=n-j+k}^{n-2} (n-\ell-1) \alpha^\ell \right).$$

403 For $j < k \leq n$,

$$404 \quad e_k^\top L^\# (e_j - e_1) = \alpha^{k-j} e_j^\top L^\# (e_j - e_1) = \frac{\alpha^{k-j}}{\sum_{\ell=0}^{n-1} \alpha^\ell} \left(\sum_{\ell=0}^{j-2} (\ell+1) \alpha^\ell \right).$$

405

406 Theorem 5.5 yields the following result.

407 COROLLARY 5.6. For $1 \leq k \leq j - 1$,

$$408 \quad (e_{k+1}^\top - e_k^\top)L^\#(e_j - e_1) = \frac{\alpha^{k-1}}{\sum_{\ell=0}^{n-1} \alpha^\ell} \left(j + \sum_{\ell=1}^{n-j} \alpha^\ell \right) > 0.$$

409 For $j \leq k \leq n - 1$, $(e_{k+1}^\top - e_k^\top)L^\#(e_j - e_1) = \frac{\alpha^{k-j}}{\sum_{\ell=0}^{n-1} \alpha^\ell} \left(\sum_{\ell=0}^{j-2} (\ell+1)\alpha^\ell \right) (\alpha - 1) > 0$.

410 Remark 5.1. Set $\tilde{L} = L + \epsilon(e_j - e_1)e_j^\top$ with $1 < j \leq n$ and $\epsilon > 0$ so that
 411 $\tilde{u} - u = -cL^\#(e_j - e_1)$ where $c = \frac{\epsilon u_j}{1 + \epsilon(L_{jj}^\# - L_{j1}^\#)} > 0$ by Theorem 4.2 b). By Theorem
 412 5.5, $\tilde{u}_1 - u_1 > 0$ and $\tilde{u}_k - u_k < 0$, $j \leq k \leq n$. It follows from Corollary 5.6 that $\tilde{u}_k - u_k$
 413 is decreasing in k if $\alpha > 1$. If $\alpha = 1$, $\tilde{u}_k - u_k$ is decreasing in k for $1 \leq k \leq j$ and
 414 constant for $j \leq k \leq n$.

415 Next we consider $L^\#(e_j - e_i)$ for $j, i > 1$. The proofs again rely on (4.7) and our
 416 expression for B^{-1} .

417 LEMMA 5.7. For a path network with $2 \leq i < j \leq n$,

$$418 \quad e_k^\top B^{-1}(e_{j-1} - e_{i-1}) = \begin{cases} 0, & \text{if } 1 \leq k \leq i - 1, \\ \sum_{\ell=0}^{k-i} \alpha^\ell, & \text{if } i - 1 < k \leq j - 1, \\ \alpha^{k-j+1} \sum_{\ell=0}^{j-i} \alpha^\ell, & \text{if } j - 1 < k \leq n, \end{cases}$$

419 THEOREM 5.8. On a path network, if $2 \leq i < j \leq n$, then

$$420 \quad e_k^\top L^\#(e_j - e_i) = -\frac{\alpha^{k-1}}{\sum_{\ell=0}^{n-1} \alpha^\ell} \left((j-i) \sum_{\ell=0}^{n-j} \alpha^\ell + \sum_{\ell=n-j+1}^{n-i-1} (n-i-\ell)\alpha^\ell \right)$$

421 for $1 \leq k \leq i$. For $i < k \leq j$,

$$422 \quad e_k^\top L^\#(e_j - e_i) = \frac{1}{\sum_{\ell=0}^{n-1} \alpha^\ell} \left(\sum_{\ell=0}^{k-i-1} (\ell+1)\alpha^\ell + (k-i) \sum_{\ell=k-i}^{k-2} \alpha^\ell \right. \\ 423 \quad \left. - (j-k) \sum_{\ell=k-1}^{n+k-j-1} \alpha^\ell - \sum_{\ell=n-j+k}^{n-2} (n-1-\ell)\alpha^\ell \right).$$

424 For $j < k \leq n$, $e_k^\top L^\#(e_j - e_i) = \alpha^{k-j} e_j^\top L^\#(e_j - e_i) = \frac{\alpha^{k-j}}{\sum_{\ell=0}^{n-1} \alpha^\ell} \left(\sum_{\ell=0}^{j-i-1} (\ell+1)\alpha^\ell \right. \\ 425 \quad \left. + (j-i) \sum_{\ell=j-i}^{j-2} \alpha^\ell \right).$

426 COROLLARY 5.9. If $2 \leq i < j \leq n$, then $(e_{k+1} - e_k^\top)L^\#(e_j - e_i) =$

$$427 \quad \begin{cases} -\frac{\alpha^{k-1}}{\sum_{\ell=0}^{n-1} \alpha^\ell} \left((j-i) \sum_{\ell=0}^{n-j} \alpha^\ell + \sum_{\ell=n-j+1}^{n-i-1} (n-i-\ell)\alpha^\ell \right) (\alpha - 1) \geq 0, & 1 \leq k \leq i - 1, \\ \frac{1}{\sum_{\ell=0}^{n-1} \alpha^\ell} \left(\sum_{\ell=0}^{i-2} \alpha^\ell + (j-i+1)\alpha^{i-1} + \sum_{\ell=i}^{n+i-j-1} \alpha^\ell \right) > 0, & k = i, \\ \frac{1}{\sum_{\ell=0}^{n-1} \alpha^\ell} \left(\sum_{\ell=k-i}^{k-2} \alpha^\ell + (j-i+1)\alpha^{k-1} + \sum_{\ell=k}^{n+k-j-1} \alpha^\ell \right) > 0, & i < k \leq k+1 \leq j, \\ \frac{\alpha^{k-j}}{\sum_{\ell=0}^{n-1} \alpha^\ell} \left(\sum_{\ell=0}^{j-2} (\ell+1)\alpha^\ell \right) (\alpha - 1) \geq 0, & j \leq k \leq n - 1. \end{cases}$$

428 *Remark 5.2.* Let $2 \leq i < j \leq n$ and $\epsilon > 0$. Set $\tilde{L} = L + \epsilon(e_j - e_i)e_j^\top$. It follows
429 from Theorem 4.2 b) that

$$430 \quad (5.7) \quad \tilde{u} - u = -cL^\#(e_j - e_i)$$

431 where $c = \frac{\epsilon u_j}{1 + \epsilon(L_{jj}^\# - L_{ji}^\#)} > 0$ (observe that $L_{jj}^\# - L_{ji}^\# > 0$ by (4.8)). In view of Theorem
432 5.8, we see that

$$433 \quad \tilde{u}_k - u_k = \begin{cases} \frac{c\alpha^{k-1}}{\sum_{\ell=0}^{n-1} \alpha^\ell} \left((j-i) \sum_{\ell=0}^{n-j} \alpha^\ell + \sum_{\ell=0}^{n-i-1} (n-i-\ell) \alpha^\ell \right) > 0, & 1 \leq k \leq i, \\ \frac{-c\alpha^{k-j}}{\sum_{\ell=0}^{n-1} \alpha^\ell} \left(\sum_{\ell=0}^{j-i-1} (\ell+1) \alpha^\ell + (j-i) \sum_{\ell=j-i}^{j-2} \alpha^\ell \right) < 0, & j \leq k \leq n. \end{cases}$$

434 Observe that if $i \geq 2$ and $1 \leq k \leq n-1$, $(\tilde{u}_{k+1} - u_{k+1}) - (\tilde{u}_k - u_k) = -c(e_{k+1} -$
435 $e_k^\top)L^\#(e_j - e_i)$. It now follows from Corollary 5.9 that if $\alpha > 1$, then $(\tilde{u}_{k+1} - u_{k+1}) -$
436 $(\tilde{u}_k - u_k) < 0$. Hence, if $\alpha > 1$ then $\tilde{u}_k - u_k$ is decreasing as a function of k for
437 $1 \leq k \leq n$.

438 Assume that a new arc from vertex j to vertex i is added, where $i < j$; the
439 following result shows that the network risk u_k decreases at all vertices downstream
440 from j and increases at all vertices upstream from i . The result follows readily from
441 Theorems 4.2 and 5.8.

442 **THEOREM 5.10.** *Consider a path network, and suppose that $1 \leq i < j \leq n$. For*
443 *any $k \leq i$, $\text{sgn}(\frac{du_k}{dm_{ji}}) < 0$, while for any $j < k$, $\text{sgn}(\frac{du_k}{dm_{ji}}) > 0$.*

444 For the vertices k between j and i (i.e., $i < k < j$), the change of the network
445 risk u_k depends on the position of the vertices as well as the magnitude of m_{ij} .

446 We now revisit the toy model of a path graph network described in section 1.

447 **EXAMPLE 1.** *In this example we show how the results developed in section 4 yield*
448 *insight into the toy example presented in Figure 1. We suppose that the time scale of*
449 *movement greatly exceeds that of the disease dynamics, so that the asymptotic approx-*
450 *imation $\mathcal{R}_0 = \sum_{k=1}^4 u_k q_k$ applies, where u denotes the null vector of the Laplacian*
451 *matrix L , normalised so that $\sum_{k=1}^4 u_k = 1$. Taking $\alpha = 1$ yields*

$$452 \quad L = \begin{bmatrix} 1 & -1 & 0 & 0 \\ -1 & 2 & -1 & 0 \\ 0 & -1 & 2 & -1 \\ 0 & 0 & -1 & 1 \end{bmatrix}, \text{ and } L^\# = \frac{1}{8} \begin{bmatrix} 7 & 1 & -3 & -5 \\ 1 & 3 & -1 & -3 \\ -3 & -1 & 3 & 1 \\ -5 & -3 & 1 & 7 \end{bmatrix}. \text{ A bypass from}$$

453 vertex 1 to vertex 3 corresponds to the perturbing matrix $E = m_{31}(e_1 - e_3)e_1^\top$, and
454 a computation now reveals that the normalised null vector of the perturbed Laplacian

$$455 \quad \text{matrix is given by } \tilde{u} = \frac{1}{4} \mathbb{1} - \frac{m_{31}}{16+20m_{31}} \begin{bmatrix} 5 \\ 1 \\ -3 \\ -3 \end{bmatrix}. \text{ If the hot spot is at vertex 2, with}$$

456 $q_i = q, i = 1, 3, 4, q_2 = 10q$, then $\mathcal{R}_0 = \sum_{k=1}^4 \tilde{u}_k q_k = q(\frac{13}{4} - \frac{9m_{31}}{16+20m_{31}})$; evidently this
457 is decreasing and concave down as a function of m_{31} , as is clearly reflected in Figure
458 1 (left plot) by computing \mathcal{R}_0 numerically.

459 Next, considering a bypass from vertex 2 to vertex 4, (so that E is given by

$$460 \quad m_{42}(e_2 - e_4)e_2^\top) \text{ an analogous argument shows that } \tilde{u} = \frac{1}{4} \mathbb{1} - \frac{m_{42}}{16+12m_{42}} \begin{bmatrix} 3 \\ 3 \\ -1 \\ -5 \end{bmatrix}.$$

461 With vertex 3 as the hot spot and $q_i = q, i = 1, 2, 4, q_3 = 10q$, it now follows that
 462 $\sum_{k=1}^4 \tilde{u}_k q_k = q(\frac{13}{4} + \frac{9m_{42}}{16+12m_{42}})$. Evidently this last is increasing and concave down as
 463 a function of m_{42} , as depicted in Figure 1 (right plot).

464 Alternatively, as u_k encodes the weights of spanning in-trees rooted at k , as shown
 465 in section 3, both bypasses (from vertex 1 to vertex 3 or from vertex 2 to vertex 4)
 466 increase u_1 and u_2 but decrease u_3 and u_4 . For example, with the bypass from vertex
 467 1 to vertex 3 of weight m_{31} , we have

$$\begin{aligned}
 468 \quad u_1 &= \frac{m_{12}m_{23}m_{34}}{\Delta} = \frac{1}{4 + 5m_{31}} = \frac{1}{4} - \frac{\frac{5}{4}m_{31}}{4 + 5m_{31}}, \\
 469 \quad u_2 &= \frac{m_{21}m_{23}m_{34} + m_{23}m_{31}m_{34}}{\Delta} = \frac{1 + m_{31}}{4 + 5m_{31}} = \frac{1}{4} - \frac{\frac{1}{4}m_{31}}{4 + 5m_{31}}, \\
 470 \quad u_3 &= \frac{m_{34}m_{32}m_{21} + m_{34}m_{31}m_{12} + m_{34}m_{31}m_{32}}{\Delta} = \frac{1 + 2m_{31}}{4 + 5m_{31}} = \frac{1}{4} + \frac{\frac{3}{4}m_{31}}{4 + 5m_{31}}, \\
 471 \quad u_4 &= \frac{m_{43}m_{32}m_{21} + m_{43}m_{32}m_{31} + m_{43}m_{31}m_{12}}{\Delta} = \frac{1 + 2m_{31}}{4 + 5m_{31}} = \frac{1}{4} + \frac{\frac{3}{4}m_{31}}{4 + 5m_{31}}, \\
 472
 \end{aligned}$$

473 where Δ is the sum of weights of spanning in-trees rooted at any vertex, that is, $\Delta =$
 474 $m_{12}m_{23}m_{34} + m_{21}m_{23}m_{34} + m_{23}m_{31}m_{34} + m_{34}m_{32}m_{21} + m_{34}m_{31}m_{12} + m_{34}m_{31}m_{32} +$
 475 $m_{43}m_{32}m_{21} + m_{43}m_{32}m_{31} + m_{43}m_{31}m_{12} = 4 + 5m_{31}$. A location of a hot spot at
 476 vertex 1 or 2 leads to the decrease of \mathcal{R}_0 due to the bypass, while a hot spot at vertex
 477 3 or 4 leads to the increase of \mathcal{R}_0 .

478 **EXAMPLE 2.** Consider a path network on 5 vertices with an additional arc from
 479 vertex 2 to vertex 4 being added. All other settings are the same as in Example 1.
 480 Figure 3 shows how \mathcal{R}_0 responds to this addition in the scenarios of the disease hot
 481 spot, located at various different vertices. It turns out that when vertex 3 is the hot
 482 spot, there is no change in \mathcal{R}_0 , no matter how large the value of m_{24} is. When the
 483 time scale of movement greatly exceeds that of the disease dynamics, the results of
 484 sections 3 and 4 explain Figure 3. For example, the bypass decreases u_1 and u_2 but
 485 increases u_4 and u_5 . Therefore, a hot spot at vertex 1 or 2 leads to a decrease of \mathcal{R}_0
 486 while a hot spot at vertex 3 or 4 leads to an increase of \mathcal{R}_0 , due to the bypass.

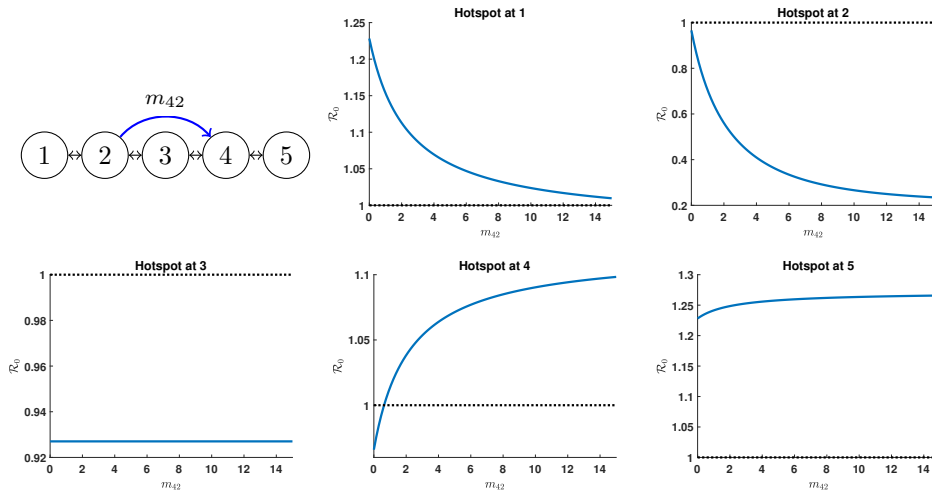


FIG. 3. The impact of a bypass in a path network of 5 vertices.

487 Motivated by the observation made in Example 2 for the case that vertex 3 is
 488 the hot spot, we use the exact network basic reproduction number to prove a general
 489 result below, from which the observation is readily recovered.

490 **THEOREM 5.11.** *Suppose that M is an irreducible movement matrix and that L*
 491 *is the corresponding Laplacian matrix. Let $c > 0$ and $V = L + cI$. Suppose further*
 492 *that there is a permutation matrix Q and indices i, j such that: a) F and L both*
 493 *commute with Q , and b) $Qe_j = e_i$. Then for any $\epsilon > 0$, the basic reproduction numbers*
 494 *corresponding to M and $M + \epsilon(e_j - e_i)e_j^\top$ are equal.*

495 *Proof.* Let $E = \epsilon(e_j - e_i)e_j^\top$. The network basic reproduction number correspond-
 496 ing to M is $\rho(FV^{-1})$, while that corresponding to the perturbed network $M + E$ is
 497 $\rho(F(V + E)^{-1})$. We have

$$498 \quad (5.8) \quad F(V + E)^{-1} = FV^{-1} \left(I + \epsilon(e_j - e_i)e_j^\top V^{-1} \right)^{-1}.$$

499 Observe that V is a column diagonally dominant M-matrix. From Lemma 3.14
 500 in Chapter 9 of [5], it follows that the maximum entry in any row of V^{-1} occurs on
 501 the diagonal. In particular, $e_j^\top V^{-1}(e_j - e_i) \geq 0$. It now follows that

$$502 \quad (5.9) \quad \left(I + \epsilon(e_j - e_i)e_j^\top V^{-1} \right)^{-1} = I - \frac{\epsilon}{1 + \epsilon e_j^\top V^{-1}(e_j - e_i)} (e_j - e_i)e_j^\top V^{-1}.$$

503 Substituting (5.9) into (5.8) yields

$$504 \quad F(V + E)^{-1} = FV^{-1} \left[I - \frac{\epsilon}{1 + \epsilon e_j^\top V^{-1}(e_j - e_i)} (e_j - e_i)e_j^\top V^{-1} \right]$$

$$505 \quad = FV^{-1} - \frac{\epsilon FV^{-1}(e_j - e_i)e_j^\top V^{-1}}{1 + \epsilon e_j^\top V^{-1}(e_j - e_i)}.$$

507 Next, consider a positive left Perron vector y for FV^{-1} , i.e. $y^\top FV^{-1} = \mathcal{R}_0 y^\top$.
 508 Since F and V both commute with Q , so does FV^{-1} . Consequently, $y^\top QFV^{-1}Q^\top =$
 509 $\mathcal{R}_0 y^\top$, implying that $(y^\top Q)FV^{-1} = \mathcal{R}_0 (y^\top Q)$. Hence $y^\top Q$ is also a left Perron vector
 510 for FV^{-1} . Since that Perron vector is unique up to a scalar multiple, we find that
 511 necessarily $y^\top Q = y^\top$. In particular, $y_i = y^\top Qe_j = y^\top e_j = y_j$.

512 Now consider

$$513 \quad y^\top F(V + E)^{-1} = y^\top FV^{-1} - \frac{\epsilon y^\top FV^{-1}(e_j - e_i)e_j^\top V^{-1}}{1 + \epsilon e_j^\top V^{-1}(e_j - e_i)}$$

$$514 \quad = \mathcal{R}_0 y^\top - \frac{\epsilon \mathcal{R}_0 (y_j - y_i)e_j^\top V^{-1}}{1 + \epsilon e_j^\top V^{-1}(e_j - e_i)} = \mathcal{R}_0 y^\top.$$

516 Hence y is a positive left eigenvector of $F(V + E)^{-1}$, (with corresponding eigen-
 517 value \mathcal{R}_0), from which it follows that $F(V + E)^{-1}$ has y as a left Perron vector and
 518 \mathcal{R}_0 as its Perron value. \square

519 *Remark 5.3.* Inspecting the proof of Theorem 5.11, we find that the conclusion
 520 holds also for negative values of ϵ , provided that $\epsilon > -m_{ij}$ and $\epsilon > -\frac{1}{e_j^\top V^{-1}(e_j - e_i)}$.

521 As an application of Theorem 5.11, consider a river network on $2k + 1$ vertices
 522 with $\alpha = 1$, and suppose that F is the diagonal matrix whose ℓ -th diagonal entry is
 523 1 for $\ell \neq k + 1$, and whose $k + 1$ -st diagonal entry is $x > 1$. Setting $V = L + cI$ for

524 some $c > 0$, we see that V and F commute with the “back diagonal” permutation
 525 matrix P , where the $(\ell, 2k + 2 - \ell)$ entry of P is 1 for $\ell = 1, \dots, 2k + 1$. Fix an index
 526 $j = 1, \dots, 2k + 1$, and note that $Pe_j = e_{2k+2-j}$. From the above theorem, for any
 527 $\epsilon > 0$, the basic reproduction numbers associated with the movement matrices M and
 528 $M + \epsilon(e_j - e_{2k+2-j})e_j^\top$ are equal. In particular, for a river network on 5 vertices with
 529 $\alpha = 1$, adding a weighted arc from vertex 4 to vertex 2 does not affect the value of \mathcal{R}_0 .
 530 This justifies the observation made in Example 2 for the hot spot locating at vertex
 531 3.

532 **6. Control strategies.** The techniques developed in sections 3 and 4 inform
 533 a strategy for controlling invasibility. Given an irreducible movement matrix M ,
 534 the control strategy corresponds to a perturbation of M , say $M + E$ which is also
 535 irreducible and nonnegative. Denoting the corresponding Laplacian matrices and
 536 normalized right null vectors by L, u and \tilde{L}, \tilde{u} respectively, we find that the associated
 537 network basic reproduction numbers are approximately $\mathcal{R}_0 = \sum_{k=1}^n u_k \mathcal{R}_0^{(k)}$ and $\tilde{\mathcal{R}}_0 =$
 538 $\sum_{k=1}^n \tilde{u}_k \mathcal{R}_0^{(k)}$. Our goal is then to find a suitable perturbing matrix E so as to ensure
 539 that $\tilde{\mathcal{R}}_0 - \mathcal{R}_0$ is negative and, ideally, large in absolute value.

540 From the results in section 4, we find that

$$541 \quad (6.1) \quad \tilde{\mathcal{R}}_0 - \mathcal{R}_0 = \sum_{k=1}^n (\tilde{u}_k - u_k) \mathcal{R}_0^{(k)} = \sum_{k=1}^n e_k^\top ((I + L^\# E)^{-1} - I) u \mathcal{R}_0^{(k)}.$$

542 In particular, for a perturbing matrix E , the effectiveness of the corresponding control
 543 strategy in mitigating the invasion can be quantified using (6.1).

544 In this section, we focus on a restricted set of perturbations: for distinct indices
 545 i, j and fixed ϵ , we consider the effect of increasing the movement rate from patch j
 546 to patch i from m_{ij} to $m_{ij} + \epsilon$. In this case, (6.1) simplifies considerably: from the
 547 results of section 4, it follows that in this restricted setting,

$$548 \quad (6.2) \quad \tilde{\mathcal{R}}_0 - \mathcal{R}_0 = - \frac{\epsilon u_j}{1 + \epsilon(L_{jj}^\# - L_{ji}^\#)} \sum_{k=1}^n (L_{kj}^\# - L_{ki}^\#) \mathcal{R}_0^{(k)}.$$

549 Our challenge is then to select the indices i, j so as to minimize the expression

$$550 \quad (6.3) \quad - \frac{\epsilon u_j}{1 + \epsilon(L_{jj}^\# - L_{ji}^\#)} \sum_{k=1}^n (L_{kj}^\# - L_{ki}^\#) \mathcal{R}_0^{(k)}.$$

551 We remark here that for $\epsilon > 0$, the expression (6.2) is always valid. However, for
 552 negative values of ϵ , another hypothesis is required in order for the derivation of
 553 (6.2) to hold. In that case, we need to assume that $-m_{ij} < \epsilon$ (otherwise there is a
 554 danger that the network is no longer strongly connected). Evidently that additional
 555 hypothesis is satisfied if, for example, we assume that when ϵ is negative, its absolute
 556 value is sufficiently small. For ease of exposition in the sequel, we only deal with the
 557 case $\epsilon > 0$ in the remainder of this section.

558 While we focus only on perturbing a single entry in the movement matrix M , note
 559 that these special perturbations are building blocks: any admissible perturbation can
 560 be written as a linear combination of these restricted perturbations.

561 From (6.3) it is clear that the specific values of $\mathcal{R}_0^{(k)}, k = 1, \dots, n$ are needed
 562 in order to assess the effect on the basic reproduction number of changing m_{ij} to
 563 $m_{ij} + \epsilon$. However, we restrict ourselves to the following situation, in which the anal-
 564 ysis simplifies even further. Imagine that one patch, say ℓ , is a “hot spot” for the

565 disease, and that the patch reproduction numbers $\mathcal{R}_0^{(k)}, k \neq \ell$ take on a common
 566 value. Formally we assume that for some index ℓ , we have $\mathcal{R}_0^{(k)} = r_0$ whenever $k \neq \ell$,
 567 with $\mathcal{R}_0^{(\ell)} > r_0$. Then $\tilde{\mathcal{R}}_0 - \mathcal{R}_0 = \sum_{k=1, \dots, n, k \neq \ell} (\tilde{u}_k - u_k) \mathcal{R}_0^{(k)} + (\tilde{u}_\ell - u_\ell) \mathcal{R}_0^{(\ell)} =$
 568 $r_0 \sum_{k=1, \dots, n, k \neq \ell} (\tilde{u}_k - u_k) + (\tilde{u}_\ell - u_\ell) \mathcal{R}_0^{(\ell)}$. The fact that $\sum_{k=1}^n (\tilde{u}_k - u_k) = 0$, gives

$$569 \quad (6.4) \quad \tilde{\mathcal{R}}_0 - \mathcal{R}_0 = (\tilde{u}_\ell - u_\ell) (\mathcal{R}_0^{(\ell)} - r_0).$$

570 For our restricted family of perturbations, we have $\tilde{\mathcal{R}}_0 - \mathcal{R}_0 = -\frac{\epsilon u_j}{1 + \epsilon(L_{jj}^\# - L_{ji}^\#)} (L_{\ell j}^\# -$
 571 $L_{\ell i}^\#) (\mathcal{R}_0^{(\ell)} - r_0)$. Hence it suffices to select the indices i, j that maximize the expres-
 572 sion $\frac{u_j}{1 + \epsilon(L_{jj}^\# - L_{ji}^\#)} (L_{\ell j}^\# - L_{\ell i}^\#)$. In subsections 6.1 and 6.2, we revisit the star and river
 573 networks and discuss how these perturbations affect the basic reproduction number.

574 **6.1. Star with a hot spot.** In what follows, we assume that $\epsilon > 0$, and we con-
 575 sider a special case. We assume that $m_{12} \geq m_{13} \geq \dots \geq m_{1n}$, and impose the further
 576 assumption that $m_{1k} = m_{k1}, k = 2, \dots, n$. We note that when this is the case, $u = \frac{1}{n} \mathbb{1}$.
 577

578 *Case 1: the hot spot is located at the hub (vertex 1):*

579 We claim that the best strategy to reduce the infection risk is to increase m_{n1} when
 580 $m_{1k} = m_{k1}$ for $2 \leq k \leq n$. Perturb $m_{1j} \rightarrow m_{1j} + \epsilon$ for $\epsilon > 0$ and $1 < j \leq n$. Then

$$581 \quad \tilde{u}_1 - u_1 = -\frac{\epsilon u_j e_1^\top L^\# (e_j - e_1)}{1 + \epsilon e_j^\top L^\# (e_j - e_1)} = \frac{\epsilon u_1 u_j \bar{\mathbb{1}}^\top B^{-1} e_{j-1}}{1 + \epsilon e_{j-1} (B^{-1} e_{j-1} - \bar{u} \bar{\mathbb{1}}^\top B^{-1} e_{j-1})}$$

$$582 \quad = \frac{\epsilon u_1 u_j / m_{1j}}{1 + \epsilon (1 - u_j) / m_{1j}} > 0.$$

583 Perturb $m_{i1} \rightarrow m_{i1} + \epsilon$ for $1 < i \leq n$. Since $B^{-1} = \text{diag}(m_{12}, \dots, m_{1n})$,

$$584 \quad \tilde{u}_1 - u_1 = -\frac{\epsilon u_1 e_1^\top L^\# (e_1 - e_i)}{1 + \epsilon e_1^\top L^\# (e_1 - e_i)} = \frac{\epsilon u_1 e_1^\top L^\# (e_i - e_1)}{1 - \epsilon e_1^\top L^\# (e_i - e_1)} = \frac{-\epsilon u_1^2 \bar{\mathbb{1}}^\top B^{-1} e_{i-1}}{1 + \epsilon u_1 \bar{\mathbb{1}}^\top B^{-1} e_{i-1}}$$

$$585 \quad = -\frac{\epsilon u_1^2 / m_{1i}}{1 + \epsilon u_1 / m_{1i}} < 0.$$

586 Since $u = \frac{1}{n} \mathbb{1}$, this gives $\tilde{u}_1 - u_1 = -\frac{1}{n} \frac{\epsilon / (nm_{1i})}{1 + \epsilon / (nm_{1i})}$. Since m_{1n} is the smallest among
 587 $\{m_{1k} : 2 \leq k \leq n\}$, the minimum of $\tilde{u}_1 - u_1$ is achieved at $k = n$, i.e.,

$$588 \quad \min_{2 \leq k \leq n} (\tilde{u}_1 - u_1) = -\frac{1}{n} \frac{\epsilon / (nm_{1n})}{1 + \epsilon / (nm_{1n})}.$$

589 This result indicates that the optimal strategy to reduce the infection risk is to increase
 590 m_{n1} when $m_{1k} = m_{k1}$ for all k .

591 Additionally, we claim that, in this special case where only changing weights
 592 between leaves is permitted, then the best strategy is to increase m_{n2} , as we now
 593 show. Perturbing $m_{ij} \rightarrow m_{ij} + \epsilon$ for $2 \leq i \neq j \leq n$, we find that

$$594 \quad (6.5) \quad \tilde{u}_1 - u_1 = -\frac{\epsilon u_j e_1^\top L^\# (e_j - e_i)}{1 + \epsilon e_j^\top L^\# (e_j - e_i)}$$

$$= \frac{\epsilon u_1 u_j \bar{\mathbb{1}}^\top B^{-1} (e_{j-1} - e_{i-1})}{1 + \epsilon e_{j-1}^\top [B^{-1} (e_{j-1} - e_{i-1}) - \bar{u} \bar{\mathbb{1}}^\top B^{-1} (e_{j-1} - e_{i-1})]}$$

$$= \frac{\epsilon \frac{1}{n^2} \left(\frac{1}{m_{1j}} - \frac{1}{m_{1i}} \right)}{1 + \epsilon \left(\frac{1}{m_{1j}} - \frac{1}{n} \left(\frac{1}{m_{1j}} - \frac{1}{m_{1i}} \right) \right)} = \frac{\epsilon \frac{1}{n^2} (m_{1i} - m_{1j})}{m_{1i} m_{1j} + \epsilon \frac{1}{n} ((n-1)m_{1i} + m_{1j})}.$$

595 Note that $\tilde{u}_1 - u_1 < 0$ only if $i > j$ and hence this is the only interesting case.

596 It is straightforward to show that $\frac{\epsilon \frac{1}{n^2} (m_{1i} - m_{1j})}{m_{1i} m_{1j} + \epsilon \frac{1}{n} ((n-1)m_{1i} + m_{1j})}$ is increasing
 597 in m_{1i} and decreasing in m_{1j} . Thus the minimum is obtained at $i = n$ and $j = 2$.

598 Hence, $\min_{1 \leq j < i \leq n} (\tilde{u}_1 - u_1) = \frac{\epsilon \frac{1}{n^2} (m_{1n} - m_{12})}{m_{1n} m_{12} + \epsilon \frac{1}{n} ((n-1)m_{1n} + m_{12})}$ which implies that
 599 the most effective strategy to reduce the risk of infection is to increase m_{n2} .

600

601 *Case 2: the hot spot is located on a leaf (vertex $\ell \neq 1$):*

602 We claim that the best strategy is to increase m_{1n} when $\frac{m_{1\ell}}{m_{1n}} > n - 1$ and $n \neq \ell$, and
 603 to increase $m_{1\ell}$ when $\frac{m_{1\ell}}{m_{1n}} < n - 1$, as we now show. Perturbing $m_{1\ell} \rightarrow m_{1\ell} + \epsilon$ yields

$$\begin{aligned} \tilde{u}_\ell - u_\ell &= -\frac{\epsilon u_\ell e_\ell^\top L^\#(e_\ell - e_1)}{1 + \epsilon e_\ell^\top L^\#(e_\ell - e_1)} = -\frac{\epsilon u_\ell e_{\ell-1}^\top (B^{-1}e_{\ell-1} - \bar{u} \bar{\mathbb{1}}^\top B^{-1}e_{\ell-1})}{1 + \epsilon e_{\ell-1}^\top (B^{-1}e_{\ell-1} - \bar{u} \bar{\mathbb{1}}^\top B^{-1}e_{\ell-1})} \\ (6.6) \quad &= -\frac{\epsilon u_\ell (1 - u_\ell) / m_{1\ell}}{1 + \epsilon (1 - u_\ell) / m_{1\ell}} = -\frac{1}{n} \frac{\epsilon \frac{n-1}{n} \frac{1}{m_{1\ell}}}{1 + \epsilon \frac{n-1}{n} \frac{1}{m_{1\ell}}} < 0. \end{aligned}$$

605 Perturbing $m_{i1} \rightarrow m_{i1} + \epsilon$ leads to

$$\tilde{u}_\ell - u_\ell = -\frac{\epsilon u_1 e_\ell^\top L^\#(e_1 - e_i)}{1 + \epsilon e_1^\top L^\#(e_1 - e_i)} = \frac{\epsilon u_1 e_\ell^\top L^\#(e_i - e_1)}{1 - \epsilon e_1^\top L^\#(e_i - e_1)}.$$

607 Hence, if $i \neq \ell$, $\tilde{u}_\ell - u_\ell = \frac{\epsilon u_1 e_{\ell-1}^\top (B^{-1}e_{i-1} - \bar{u} \bar{\mathbb{1}}^\top B^{-1}e_{i-1})}{1 + \epsilon u_1 \bar{\mathbb{1}}^\top B^{-1}e_{i-1}} = -\frac{1}{n} \frac{\frac{\epsilon}{n} \frac{1}{m_{1i}}}{1 + \frac{\epsilon}{n} \frac{1}{m_{1i}}} < 0$,

608 and if $i = \ell$, $\tilde{u}_\ell - u_\ell = \frac{\epsilon u_1 e_{\ell-1}^\top (B^{-1}e_{\ell-1} - \bar{u} \bar{\mathbb{1}}^\top B^{-1}e_{\ell-1})}{1 + \epsilon u_1 \bar{\mathbb{1}}^\top B^{-1}e_{\ell-1}} = \frac{n-1}{n} \frac{\frac{\epsilon}{n} \frac{1}{m_{1\ell}}}{1 + \frac{\epsilon}{n} \frac{1}{m_{1\ell}}} > 0$. If

609 $i \neq \ell$, then the minimum of $\tilde{u}_\ell - u_\ell$ is achieved at $i = n$. To compare the two different
 610 strategies (i.e., $m_{1\ell}$ and m_{n1}), we have the following conclusion: If $m_{1\ell}/m_{1n} < n - 1$,
 611 the most effective strategy is to increase $m_{1\ell}$; If $m_{1\ell}/m_{1n} > n - 1$, the most effective
 612 strategy is to increase m_{1n} provided that $n \neq \ell$.

613 **6.2. River with a hot spot.** As in section 6.1, we introduce a simplifying
 614 hypothesis in order to make the analysis more tractable. We assume that $\alpha = 1$ (i.e.,
 615 $a = b$), and observe that when this is the case, $u = \frac{1}{n} \mathbb{1}$.

616 We now have the following result.

617 **LEMMA 6.1.** *Suppose that $1 \leq i < j \leq n$. If $\alpha = 1$, then*

$$e_k^\top L^\#(e_j - e_i) = \begin{cases} -\frac{1}{2n}(j-i)(2n-i-j+1), & 1 \leq k \leq i, \\ (k-j) + \frac{1}{2n}(j-i)(i+j-1), & i < k \leq j, \\ \frac{1}{2n}(j-i)(i+j-1), & j < k \leq n. \end{cases}$$

619 *Remark 6.1.* By Lemma 6.1 and equation (5.7), it is clear that $\tilde{u}_k - u_k$ is a
 620 continuous, piecewise linear function and decreasing in k for $1 \leq k \leq n$. For $1 \leq k \leq i$,
 621 $\tilde{u}_k - u_k$ is positive and constant in k , while for $j \leq k \leq n$, $\tilde{u}_k - u_k$ is negative and
 622 constant in k .

623 Assume that $1 \leq i < j \leq n$. By (6.4), to minimize the infection risk, it suffices
 624 to minimize $\tilde{u}_\ell - u_\ell$. Perturb $m_{ij} \rightarrow m_{ij} + \epsilon$ with $\epsilon > 0$. We have

$$\tilde{u}_\ell - u_\ell = -\frac{\epsilon u_j e_\ell^\top L^\#(e_j - e_i)}{1 + \epsilon(L_{jj}^\# - L_{ji}^\#)} := -u_j g(i, j).$$

626 When $\alpha = 1$, $u_i = \frac{1}{n}$ for all $1 \leq i \leq n$ and $\min_{i,j}(\tilde{u}_\ell - u_\ell) = -\frac{1}{n} \max_{i,j} g(i, j)$.
 627 Minimizing $\tilde{R}_0 - R_0$ is equivalent to maximizing $g(i, j)$ over i and j for $1 \leq i < j \leq n$.
 628 It turns out that

$$\max_{i,j=1,\dots,n,i \neq j} g(i, j) = \max \left\{ \frac{\epsilon \ell(\ell - 1)}{2n + \epsilon \ell(\ell - 1)}, \frac{\epsilon(n + 1 - \ell)(n + 2 - \ell)}{2n + \epsilon(n + 1 - \ell)(n + 2 - \ell)} \right\}$$

629 (see the supplementary material for the details).

630 On the other hand, if $1 \leq i < j \leq n$ are fixed, by Lemma 6.1, $\min_\ell(\tilde{u}_\ell - u_\ell)$ can
 631 be achieved at any $j \leq \ell \leq n$.

632 **7. Concluding remarks.** Our study is motivated by cholera, and focuses on
 633 disease dynamics, but our results also shed new insights on many spatial ecological
 634 studies, for example, the evolution of dispersal in patchy landscapes as studied in
 635 [2, 27] in a discrete time model.

636 Our methods give qualitative and quantitative information about the behavior of
 637 the basic reproduction number \mathcal{R}_0 as the topology of the network changes, and have
 638 applications to control strategies for mitigating disease spread among the patches.
 639 Our analysis can be thought of as the introduction of connections on the network, or
 640 changing the weight of existing connections. In the case that the change in a weight
 641 is positive, we have considered optimal strategies for a star and a river network. Our
 642 formula (4.2) is valid for all positive perturbations of a network connection, but a
 643 negative perturbation must be small for this to remain valid. Optimal strategies
 644 can also be formulated for a small negative change, as long as the network remains
 645 strongly connected. The effect of breaking this strong connectivity, and thus breaking
 646 the network topology, remains to be considered.

647 In patch models, the monotonicity of \mathcal{R}_0 with respect to travel frequency or the
 648 diffusion coefficient on a static network has been studied in several papers, for ex-
 649 ample [1, 18]; by contrast our results focus on the network topology. The network
 650 threshold parameter \mathcal{R}_0 governs the invasibility of the disease, but not the final size or
 651 endemicity of an invading disease. To consider this, it is necessary to use the original
 652 dynamical model.

653

654 Acknowledgments.

655 The authors thank the American Institute of Mathematics (AIM) for its hosting
 656 and generous support of an AIM SQuaRE program focusing on epidemic dynamics of
 657 cholera in non-homogeneous environments, at which this research was initiated and
 658 developed.

659

REFERENCES

- 660 [1] L. J. S. ALLEN, B. M. BOLKER, Y. LOU, AND A. L. NEVAI, *Asymptotic profiles of the steady*
 661 *states for an SIS epidemic patch model*, SIAM J. Appl. Math., 67 (2007), pp. 1283–1309.
 662 [2] L. ALTENBERG, *Resolvent positive linear operators exhibit the reduction phenomenon*, Proc.
 663 Natl. Acad. Sci. USA, 109 (2012), pp. 3705–3710.
 664 [3] M. Y. ANWAR, J. L. WARREN, AND V. E. PITZER, *Diarrhea patterns and climate: A spatiotem-*
 665 *poral Bayesian hierarchical analysis of diarrheal disease in Afghanistan*, American Journal
 666 of Tropical Medicine and Hygiene, 101 (2019), pp. 525–533.
 667 [4] M. BAQIR, Z. A. SOBANI, A. BHAMANI, N. S. BHAM, S. ABID, J. FAROOK, AND M. A. BEG,
 668 *Infectious diseases in the aftermath of monsoon flooding in Pakistan*, Asian Pacific Journal
 669 of Tropical Biomedicine, 2 (2012), pp. 76–79.
 670 [5] A. BERMAN AND R. PLEMMONS, *Nonnegative Matrices in the Mathematical Sciences*, Society
 671 for Industrial and Applied Mathematics, Philadelphia, PA, 1994.

- 672 [6] E. BERTUZZO, L. MARI, L. RIGHETTO, M. GATTO, R. CASAGRANDE, I. RODRIGUEZ-ITURBE,
673 AND A. RINALDO, *Hydroclimatology of dual-peak annual cholera incidence: insights from*
674 *a spatially explicit model*, Geophysical Research Letters, 39 (2012).
- 675 [7] S. L. CAMPBELL AND C. D. MEYER, *Generalized Inverses of Linear Transformations*, Society
676 for Industrial and Applied Mathematics, Philadelphia, PA, 2009.
- 677 [8] R. S. CANTRELL, C. COSNER, M. A. LEWIS, AND Y. LOU, *Evolution of dispersal in spatial*
678 *population models with multiple timescales*, J. Math. Biol., Published online, <https://doi.org/10.1007/s00285-018-1302-2>.
679
- 680 [9] E. J. CARLTON, J. N. EISENBERG, J. GOLDSTICK, W. CEVALLOS, J. TROSTLE, AND K. LEVY,
681 *Heavy rainfall events and diarrhea incidence: the role of social and environmental factors*,
682 American Journal of Epidemiology, 179 (2013), pp. 344–352.
- 683 [10] M. CARREL, P. VOSS, P. K. STREATFIELD, M. YUNUS, AND M. EMCH, *Protection from an-*
684 *annual flooding is correlated with increased cholera prevalence in Bangladesh: a zero-inflated*
685 *regression analysis*, Environmental Health, 9 (2010), p. 13.
- 686 [11] S. CHAIKEN, *A combinatorial proof of the all minors matrix tree theorem*, SIAM J. Algebraic
687 Discrete Methods, 3 (1982), pp. 319–329.
- 688 [12] S. CHEN, J. SHI, Z. SHUAI, AND Y. WU, *Spectral monotonicity of perturbed quasi-positive*
689 *matrices with applications in population dynamics*, arXiv preprint arXiv:1911.02232.
- 690 [13] F. C. CURRIERO, J. A. PATZ, J. B. ROSE, AND S. LELE, *The association between extreme*
691 *precipitation and waterborne disease outbreaks in the United States, 1948–1994*, American
692 Journal of Public Health, 91 (2001), pp. 1194–1199.
- 693 [14] E. DEUTSCH AND M. NEUMANN, *On the first and second order derivatives of the perron vector*,
694 Linear Algebra Appl., 71 (1985), pp. 57–76.
- 695 [15] M. DHIMAL, B. AHRENS, AND U. KUCH, *Climate change and spatiotemporal distributions of*
696 *vector-borne diseases in Nepal—a systematic synthesis of literature*, PLOS One, 10 (2015),
697 p. e0129869.
- 698 [16] M. C. EISENBERG, G. KUJBIDA, A. R. TUIITE, D. N. FISMAN, AND J. H. TIEN, *Examining*
699 *rainfall and cholera dynamics in Haiti using statistical and dynamic modeling approaches*,
700 Epidemics, 5 (2013), pp. 197–207.
- 701 [17] M. C. EISENBERG, Z. SHUAI, J. H. TIEN, AND P. VAN DEN DRIESSCHE, *A cholera model in a*
702 *patchy environment*, Math. Biosci., 246 (2013), pp. 105–112.
- 703 [18] D.-Z. GAO, *Travel frequency and infectious diseases*, SIAM J. Appl. Math., 79 (2019), pp. 1581–
704 1606.
- 705 [19] D.-Z. GAO AND C.-P. DONG, *Fast diffusion inhibits disease outbreaks*, arXiv preprint
706 arXiv:1907.12229.
- 707 [20] M. GATTO, L. MARI, E. BERTUZZO, R. CASAGRANDE, L. RIGHETTO, I. RODRIGUEZ-ITURBE, AND
708 A. RINALDO, *Generalized reproduction numbers and the prediction of patterns in water-*
709 *borne disease*, Proceedings of the National Academy of Sciences, 109 (2012), pp. 19703–
710 19708.
- 711 [21] A. GAUDIELLO, *Mathematical Investigation of the Spatial Spread of an Infectious Disease in a*
712 *Heterogeneous Environment*, PhD thesis, University of Central Florida, 2019.
- 713 [22] S. GOURLEY, R. LIU, AND J. WU, *Spatiotemporal patterns of disease spread: Interaction of*
714 *physiological structure, spatial movements, disease progression and human intervention*,
715 in Structured Population Models in Biology and Epidemiology, Springer, 2008, pp. 165–
716 208.
- 717 [23] M. HASHIZUME, B. ARMSTRONG, S. HAJAT, Y. WAGATSUMA, A. S. FARUQUE, T. HAYASHI, AND
718 D. A. SACK, *The effect of rainfall on the incidence of cholera in Bangladesh*, Epidemiology,
719 19 (2008), pp. 103–110.
- 720 [24] R. A. HORN AND C. R. JOHNSON, *Matrix Analysis*, Cambridge University Press, Cambridge,
721 2013.
- 722 [25] S. KARLIN, *Classifications of selection-migration structures and conditions for a protected poly-*
723 *morphism*, in Evolutionary Biology, vol. 14, Plenum Press, New York, 1982, pp. 61–204.
- 724 [26] R. B. KAUL, M. V. EVANS, C. C. MURDOCK, AND J. M. DRAKE, *Spatio-temporal spillover risk*
725 *of yellow fever in Brazil*, Parasites & Vectors, 11 (2018), p. 488.
- 726 [27] S. KIRKLAND, C.-K. LI, AND S. J. SCHREIBER, *On the evolution of dispersal in patchy land-*
727 *scapes*, SIAM J. Appl. Math., 66 (2006), pp. 1366–1382.
- 728 [28] S. J. KIRKLAND AND M. NEUMANN, *Group Inverses of M–Matrices and their Applications*,
729 CRC Press, Boca Raton, FL, 2013.
- 730 [29] K. LEVY, S. M. SMITH, AND E. J. CARLTON, *Climate change impacts on waterborne diseases:*
731 *moving toward designing interventions*, Current Environmental Health Reports, 5 (2018),
732 pp. 272–282.
- 733 [30] K. LEVY, A. P. WOSTER, R. S. GOLDSTEIN, AND E. J. CARLTON, *Untangling the impacts*

- 734 *of climate change on waterborne diseases: a systematic review of relationships between*
 735 *diarrheal diseases and temperature, rainfall, flooding, and drought*, Environmental Science
 736 & Technology, 50 (2016), pp. 4905–4922.
- 737 [31] A. LÓPEZ-QUÍLEZ, *Spatio-temporal analysis of infectious diseases*, International Journal of En-
 738 vironmental Research and Public Health, 16 (2019), p. 669.
- 739 [32] M. Á. LUQUE FERNÁNDEZ, A. BAUERNFEIND, J. D. JIMÉNEZ, C. L. GIL, N. E. OMEIRI, AND
 740 D. H. GUIBERT, *Influence of temperature and rainfall on the evolution of cholera epidemics*
 741 *in Lusaka, Zambia, 2003–2006: analysis of a time series*, Transactions of the Royal Society
 742 of Tropical Medicine and Hygiene, 103 (2009), pp. 137–143.
- 743 [33] L. MARI, R. CASAGRANDE, E. BERTUZZO, A. RINALDO, AND M. GATTO, *Conditions for transient*
 744 *epidemics of waterborne disease in spatially explicit systems*, Royal Society Open Science,
 745 6 (2019), p. 181517.
- 746 [34] C. D. MEYER, *The condition of a finite markov chain and perturbation bounds for the limiting*
 747 *probabilities*, SIAM J. Algebraic Discrete Methods, 1 (1980), pp. 273–283.
- 748 [35] C. D. MEYER, *Matrix Analysis and Applied Linear Algebra*, SIAM, 2000.
- 749 [36] J. W. MOON, *Counting Labelled Trees*, Canadian Mathematical Congress, Montreal, Canada,
 750 1970.
- 751 [37] M. H. MYER AND J. M. JOHNSTON, *Spatiotemporal Bayesian modeling of West Nile virus:*
 752 *Identifying risk of infection in mosquitoes with local-scale predictors*, Science of the Total
 753 Environment, 650 (2019), pp. 2818–2829.
- 754 [38] J. OKPASUO, F. OKAFOR, AND I. AGUZIE, *Effects of household drinking water choices, knowl-*
 755 *edge, practices and spatio-temporal trend on the prevalence of waterborne diseases in*
 756 *Enugu Urban, Nigeria*, International Journal of Infectious Diseases, 73 (2018), pp. 225–226.
- 757 [39] M. G. ROSA-FREITAS, N. A. HONÓRIO, C. T. CODEÇO, G. L. WERNECK, AND N. DEGALLIER,
 758 *Spatial studies on vector-transmitted diseases and vectors*, Journal of Tropical Medicine,
 759 2012 (2012).
- 760 [40] G. ROSSI, S. KARKI, R. L. SMITH, W. M. BROWN, AND M. O. RUIZ, *The spread of mosquito-*
 761 *borne viruses in modern times: A spatio-temporal analysis of dengue and chikungunya*,
 762 Spatial and Spatio-Temporal Epidemiology, 26 (2018), pp. 113–125.
- 763 [41] M. S. SARFRAZ, N. K. TRIPATHI, T. TIPDECHO, T. THONGBU, P. KERDTHONG, AND M. SOURIS,
 764 *Analyzing the spatio-temporal relationship between dengue vector larval density and land-*
 765 *use using factor analysis and spatial ring mapping*, BMC Public Health, 12 (2012), p. 853.
- 766 [42] W. SUN, L. XUE, AND X. XIE, *Spatial-temporal distribution of dengue and climate charac-*
 767 *teristics for two clusters in Sri Lanka from 2012 to 2016*, Scientific Reports, 7 (2017),
 768 p. 12884.
- 769 [43] A. J. TATEM, D. J. ROGERS, AND S. I. HAY, *Global transport networks and infectious disease*
 770 *spread*, Advances in Parasitology, 62 (2006), pp. 293–343.
- 771 [44] J. H. TIEN, Z. SHUAI, M. C. EISENBERG, AND P. VAN DEN DRIESSCHE, *Disease invasion on*
 772 *community networks with environmental pathogen movement*, J. Math. Biol., 70 (2015),
 773 pp. 1065–1092.
- 774 [45] A. VENKAT, T. M. A. FALCONI, M. CRUZ, M. A. HARTWICK, S. ANANDAN, N. KUMAR,
 775 H. WARD, B. VEERARAGHAVAN, AND E. N. NAUMOVA, *Spatiotemporal patterns of cholera*
 776 *hospitalization in Vellore, India*, International Journal of Environmental Research and
 777 Public Health, 16 (2019), p. 4257.
- 778 [46] L. S. WALDRON, B. DIMESKI, P. J. BEGGS, B. C. FERRARI, AND M. L. POWER, *Molecular*
 779 *epidemiology, spatiotemporal analysis, and ecology of sporadic human cryptosporidiosis in*
 780 *Australia*, Appl. Environ. Microbiol., 77 (2011), pp. 7757–7765.
- 781 [47] L. A. WALLER, B. J. GOODWIN, M. L. WILSON, R. S. OSTFELD, S. L. MARSHALL, AND E. B.
 782 HAYES, *Spatio-temporal patterns in county-level incidence and reporting of lyme disease*
 783 *in the northeastern United States, 1990–2000*, Environmental and Ecological Statistics, 14
 784 (2007), p. 83.

785 **Supplementary Material.** 1. Suppose that \hat{L} is given by (5.5). We claim that it
 786 suffices to consider the case that $a \geq b$. To see the claim, first note that $\hat{L} = P\bar{L}P^\top$,
 787 where

$$788 \quad (7.1) \quad \bar{L} = \begin{pmatrix} b & -a & 0 & \cdots & 0 & 0 \\ -b & a+b & -a & \cdots & 0 & 0 \\ 0 & -b & a+b & \cdots & 0 & 0 \\ \vdots & \vdots & & & & \\ 0 & 0 & 0 & \cdots & a+b & -a \\ 0 & 0 & 0 & \cdots & -b & a \end{pmatrix}$$

789 and P is the $n \times n$ “back diagonal” permutation matrix such that $p_{j, n+1-j} = 1, j =$
 790 $1, \dots, n$. If it happens that $a < b$, we then work with \bar{L} instead of \hat{L} .
 791

792 2. Here we derive the expression for $\max_{i,j=1,\dots,n,i \neq j} g(i, j)$ given at the end of section
 793 6.2. If $1 \leq \ell \leq i$, then by Lemma 6.1, $g(i, j) = \frac{\epsilon \left[-\frac{1}{2n}(j-i)(2n-i-j+1) \right]}{1 + \epsilon \frac{1}{2n}(j-i)(i+j-1)}$. So
 794 $\max_{i,j} g(i, j)$ is achieved when $i = n-1$ and $j = n$ and $\max_{i,j} g(i, j) = -\frac{\epsilon/n}{1 + \epsilon/n}$.

795 If $j \leq \ell \leq n$, then by Lemma 6.1, $g(i, j) = \frac{\epsilon \left[\frac{1}{2n}(j-i)(i+j-1) \right]}{1 + \epsilon \frac{1}{2n}(j-i)(i+j-1)}$. Thus
 796 $\max_{i,j} g(i, j)$ is achieved when $j = \ell$ and $i = 1$.

797 For the intermediate case where $i < \ell \leq j$, using Lemma 6.1, we have

$$798 \quad g(i, j) = \frac{\epsilon \left[(\ell-j) + \frac{1}{2n}(j-i)(i+j-1) \right]}{1 + \epsilon \frac{1}{2n}(j-i)(i+j-1)} \leq \frac{\epsilon \left[\frac{1}{2n}(j-i)(i+j-1) \right]}{1 + \epsilon \frac{1}{2n}(j-i)(i+j-1)}$$

Clearly it follows from the result above that $\max_{i,j} g(i, j)$ is achieved when $j = \ell$
 and $i = 1$. Hence, if $i \leq \ell \leq n$, $\max_{i,j} g(i, j) = \frac{\epsilon \ell(\ell-1)}{2n + \epsilon \ell(\ell-1)}$. It now fol-
 lows that $\max_{1 \leq i < j \leq n} g(i, j) = \frac{\epsilon \ell(\ell-1)}{2n + \epsilon \ell(\ell-1)}$. A parallel argument (which proceeds
 by considering the indices $n+1-j, n+1-i$) shows that $\max_{1 \leq j < i \leq n} g(i, j) =$
 $\frac{\epsilon(n+1-\ell)(n+2-\ell)}{2n + \epsilon(n+1-\ell)(n+2-\ell)}$. We deduce that

$$\max_{i,j=1,\dots,n,i \neq j} g(i, j) = \max \left\{ \frac{\epsilon \ell(\ell-1)}{2n + \epsilon \ell(\ell-1)}, \frac{\epsilon(n+1-\ell)(n+2-\ell)}{2n + \epsilon(n+1-\ell)(n+2-\ell)} \right\}.$$